Cell to Cell Signaling via AKT Causes T Cell Differentiation and Collapse of Tumour Stroma

Anthony Joseph Leonardi

This introductory section is submitted in partial fulfilment of the requirements of Kingston University for the degree of Doctor of Philosophy by publication.

Kingston University, School of Life Science, Pharmacy and Chemistry

Director of Studies: Dr. Helmout Modjtahedi

April 2018

DECLARATION

I declare that no material contained in the thesis has been used in any other submission for an academic award.

I declare that all material contained in the thesis is my own original work, and that any references to or use of other sources have been clearly acknowledged within the text.

Anthony Leonardi

ABSTRACT

Adoptive Cell Therapy of cancer using T cells is entering mainstream practice after years as a research method. Central to the efficacy of this "living therapy" is the function of the T cells transferred. T-cells, like other primary tissue cells, undergo differentiation and death. Clinical and preclinical data shows that lesser differentiated, less glycolytic, and more proliferative-capable cells used for the adoptive transfer yield superior tumor responses.

This introductory section will describe discoveries which elucidate and control T-cell differentiation and function for the improvement of adoptive cell therapy. Namely by use of inhibition of the PI3k/AKT pathways, and through the discovery of a dual function of death and differentiation by the canonical death receptor Fas, which can be parsed apart with a mutation from valine to cysteine at the 194 position (C194V), differentiation can be withheld while leaving cell proliferation unhindered during T-cell stimulation and expansion. The data also reveals that the differentiation signal caused by extracellular Fas ligation passes through AKT, revealing both Fas and AKT as points of intervention for targeting differentiation along the same pathway.

From further investigation, this introduction will describe the effect of AKT inhibition on T-cell differentiation on a transciptional and metabolic level. The data reveals AKT inhibition promoted FOXO1 intranuclear organization, which creates a more naive-like phenotype to the cells, and lower glycolytic status, another phenotype associated with persistent and long-lived cells. Furthermore, this control of AKT and Fas in T-cells yields benefits in several modalities of pre-clinical models of adoptive T-cell immunotherapy of cancer, in both use of a chimeric antigen receptor (CAR) and with use of Tumor Infiltrating Lymphocytes (TIL). Finally, the real-world applicability of the finding including the use of AKT inhibition in current approved Adoptive T-cell immunotherapies will be discussed.

ACKNOWLEDGEMENTS

I would like to thank my Advisor, Professor Helmout Modjtahedi, for his support and time in the work and especially as my champion and advocate. Dr. Luca Gattinoni gave mentorship and scientific training during my time at the US National Institutes of Health (NIH) in Bethesda, Maryland. Dr. Christopher Klebanoff has fostered my development and career as a scientist. I am thankful for my employer of four years at the NIH, Dr. Nicholas Restifo, for giving me the position in the laboratory on the subject I had dreamt about since high school, Tumor Immunotherapy, and for taking me in for a fourth year of fellowship. I am the admirer of Dr. Steven Rosenberg and am thankful for the passion and dedication he carried in his oversight of the Surgery Branch of the NIH.

My personal friends and colleagues from my time at Johns Hopkins in Baltimore, Maryland USA- Dr. David Kotlyar and Dr. Rui Proenca deserve thanks. Dr. Kotlyar frequently hosted me during my stays at the NIH while I was doing projects and revision experiments, is an endless source of encouragement, and supported me in the decision to write a PhD. Dr. Proenca constantly hones my scientific acumen through our friendship and discussions. Dr. Joseph Gorodenker from Johns Hopkins gave me thoughtful criticism and guidance. Professor Ed Hedgecock from Johns Hopkins always made time to provide insight and guidance beginning from my undergraduate and masters while at Johns Hopkins, and now into PhD.

My family has given unwavering support. Bruce Simon has supported my scientific development. My mother Valerie has always lent an ear. My sister Lena gave important suggestions. My older brother Andrew Delgado and his wife Suzanne Bilderback hosted me for a month while writing, during which time I got to meet my nephew Agustin Delgado. Madison Geores has given thoughtful comments. My younger brother Matthew's frequent calls assure I am never lonely while overseas.

TABLE OF CONTENTS

Pages viii and ix removed at request from the author.

LIST OF FIGURES

LIST OF TABLES

LIST OF ABBREVIATIONS

2-DG	2-Deoxy-D-glucose
2-NBDG	2-Deoxy-2-[(7-nitro-2,1,3-benzoxadiazol-4-yl)amino]-D-glucose
4-1BB	tumour necrosis factor receptor superfamily member 9
7-AAD	7-aminoactinomycin D
A2aR	adenosine A2a receptor
AB TCR	alpha beta T cell Receptor
Ad	Adenovirus
AICD	Activation Induced Cell Death
AKT	protein kinase B
AKTi	Protein Kinase B inhibitor
ALL	acute lymphoblastic
ALPS	Autoimmune lymphoproliferative syndrome
ANOVA	Analysis of variance
APC	antigen presenting cell
ATRA	All trans retinoic acid
B16	B16 Melanoma
B6	Black 6
B7	Cluster of differentiation 80 and 86
B7RP1	B7-related protein 1
BTLA	B and T lymphocyte attenuator
C57BL/6	Black 6
CAR	Chimeric Antigen Receptor
CCR7	C-C chemokine receptor type 7
CD11b	Integrin alpha M
CD122	Interleukin-2 receptor subunit beta
CD137	tumour necrosis factor receptor superfamily member 9
CD178	Fas ligand
CD19	B-Lymphocyte Surface Antigen B4
CD27	Tumour Necrosis Factor Receptor Superfamily, Member 7
CD28	T-cell-specific surface glycoprotein
CD3	Cluster of differentiation

CD4+	Cluster of differentiation
CD40L	Tumour Necrosis Factor Receptor Superfamily Member 5
CD44	GP90 lymphocyte homing/adhesion receptor
CD45.1	Protein Tyrosine Phosphatase, Receptor Type C 1
CD45.2	Protein Tyrosine Phosphatase, Receptor Type C 2
CD45RA	Protein Tyrosine Phosphatase, Receptor Type C RA
CD45RO	Protein Tyrosine Phosphatase, Receptor Type C RO
CD52	cluster of differentiation 52
CD62L	L-selectin
CD8α	Cluster of differentiation 8 alpha
CD90.2	Cluster of differentiation 90.2
CD95	Fas/APOE/ tumour necrosis factor receptor superfamily member 6
cDNA	Circular Deoxyribonucleic acid
Cgy	centigray
CH3	Histone 3 type 1
CRISPR/Cas9	Clustered Regularly Interspaced Short Palindromic Repeats/ CRISPR associated protein 9
cRNA	Circular RNA
CRR	Complete response rate
CRS	Cytokine release syndrome
CSC	Cancer stem cells
CTLA4	cytotoxic T-lymphocyte-associated antigen 4
D-luciferin	Left luciferin
dMMR	mismatch-repair–deficient
DMOG	dimethyloxalylglycine
DMSO	Dimethyl sulfoxide
ECAR	extracellular acidification rate
ELISA	enzyme-linked immunosorbent assay
EOMES	eomesodermin
ERK	Extracellular Signal-regulated Kinase
FACS	Fluorescence-activated cell sorting
FAO	Fatty acid oxidation
FasL	Tumour Necrosis Factor (Ligand) Superfamily, Member 6
FasR	Tumour Necrosis Factor Receptor Superfamily, Member 6
FBS	Fetal bovine serum
Fc	Fragment crystallizable region
FDR	false discovery rate

FHD	forkhead domain
Flt3L	FMS-like tyrosine kinase 3 ligand
FOXO1	Forkhead box protein O1
FOXP1	Forkhead box P1
GAL9	galectin 9
GAPDH	Glyceraldehyde 3-phosphate dehydrogenase
GC/MS	Gas chromatography–mass spectrometry
GCV	Ganciclovir
GEO	Gene Expression Omnibus
Gy	Gray
Gzmb	Granzyme B
HD	Human donor
HER2	human epidermal growth factor receptor 2
hgp10025–33	Human gene pigment 10025-33
HIF-Hydroxylase	Hypoxia-inducible factor-proline dioxygenase
Hk2	Hexokinase-2
HLA-A*02	human leukocyte antigen A 02
HVEM	herpesvirus entry mediator
i.p.	intraperitoneal
ICOS	inducible T cell co-stimulator
ID	inhibitor of DNA-binding
IFNγ	interferon-γ
IGG	Immunoglobulin G
IL	interleukin
IL-12	interleukin-12
IL-15	Interleukin-15
IL-2	interleukin-2
IL-33	interleukin-33
IL-7	interleukin-7
IL-7Rα	interleukin-7 receptor alpha
IPSC	induced pluripotent stem cells
IU	International units
JCI	Journal of Clinical Investigation
K562	Human erythroleukemia line
Kcna3	Potassium voltage-gated channel, shaker-related subfamily, member 3
KIR	killer cell immunoglobulin- like receptor

KLF	Kruppel-like factor
KLRG1	killer cell lectin-like receptor subfamily G, member 1
LAG3	lymphocyte activation gene 3
LC/MS/MS	liquid chromatography/ mass spectrometry
LDHA	Lactate dehydrogenase A
LEF1	lymphoid enhancer-binding factor 1
Lpr	Lymphoproliferative
Ly5.1	Protein Tyrosine Phosphatase, Receptor Type 1
Ly5.2	Protein Tyrosine Phosphatase, Receptor Type 2
Lz-FasL	leucine zipper FasL
MAPK	Mitogen-activated protein kinase
meCAR	Memory enriched chimeric antigen receptor
MFI	Mean Fluorescence Intensity
MHC	major histocompatibility complex
miRNAs	microRNAs
ml	milliLiter
mm	millimeter
mM	milliMolar
MRL	Murphy Roths Large
mRNA	Messenger ribonucleic acid
MSCV	Murine Stem Cell Virus
MSGV	Mouse Salivary Gland virus
MSI-H	microsatellite instability–high
mTOR	mammalian Target of Rapamycin
NALM6	non-T, non-B acute lymphoblastic leukemia
NCI	National Cancer Institute
ND	not determined
NES	nuclear export signal
NIAMS	National Institute of Arthritis and Musculoskeletal and Skin Diseases
NIH	National Institutes of Health
NLS	nuclear localization signal
NOD	Non-obese diabetic
NSG	NOD scid γ
NY-ESO-1	New York Esophageal Squamous Cell Carcinoma-1
OKT3	Muromonab-CD3
ORR	Objective Response Rate
OT-1	Ovalbumin T cell-1

OX-40	Tumour necrosis factor receptor superfamily member 4
pAKT	Phosphorylated Protein kinase B
PBL	Peripheral blood lymphocyte
PBMC	peripheral blood mononuclear cell
PCA	principal component analysis
PD1	programmed cell death protein 1
PDL	PD1 ligand
PI	Propidium iodide
PI3k	Phosphatidylinositol-4,5-bisphosphate 3-kinase
Pmel-1	premelanosome protein-1
PRDM1	PR domain-containing 1
pS6	Phosphorylated Ribosomal protein S6 kinase
PTLD	Post Transplant Lymphoproliferative Disorder
Ptprca	Protein tyrosine phosphatase, receptor type, C
qPCR	quantitative polymerase chain reaction
Rag1	Recombination activating gene 1
RMA	Robust Multichip analysis
RPMI	Roswell Park Memorial Institute medium
RV	retrovirus
rVV-gp100	recombinant vaccinia virus encoding the gp100 Antigen
s.c.	subcutaneous
S1pr1	Sphingosine 1-phosphate receptor 1
S6 Kinase	Ribosomal protein S6 kinase
Sca-1	complex scaffold protein-1
scFv	single-chain variable region
SELL	L-selectin
SEM	standard error of the mean
SLC16A3	Monocarboxylate transporter 4
Slc2a1	Solute carrier family 2, facilitated glucose transporter member 1
T2A	Trichocyst matrix protein T2-A
TAD	transcriptional activation domain
TALEN	Transcription activator-like effector nucleases
TBX21	T-box 21
TBX21	T-box transcription factor 21
TCF7	T cell factor 7
Tcm	Central memory T cell
TCR	T-cell receptor

Tcrb	Tcrb T cell receptor beta chain
Td	transduction
Teff	Effector T cell
Tem	Effector memory T cells
Tfrc	transferrin receptor
TGFβ	transforming growth factor-β
Th1	helper T cells-1
TIL	Tumour infiltrating lymphocytes
TIM3	T cell membrane protein 3
TK	thymidine kinase
tm1	Tropomyosin
TMix	Naïve and efector T cells
Tn	Naïve T cell
TNF	Tumour necrosis factor
TNFR2	Tumour necrosis factor Receptor 2
Treg	T regulatory cell
TRP-1	tyrosinase related protein-1
Tscm	Memory stem cell
ug	microgram
ul	microliter
uM	micromolar
veh	vehicle
Vγ9Vδ2	Vgamma9Vdelta2 T cells
WT	Wild type
ZEB2	zinc finger E-box binding homeobox 2
ZNF domain	Zinc finger domain
αFasL	anti-FasL

1 INTRODUCTION

The acquisition of T cell effector function is believed to be a predominantly multifactorial process, dependent upon a number of variables working within a context where effector function is necessary following TCR ligation and receptor costimulation (Gattinoni and Klebanoff, 2012). Elucidation of the differentiation process is important as it would enable control of T cell physiology for several purposes, applicable to a wide range of fields concerned with tumour biology and immunity alike. For example, control of a cell's differentiation status would allow for the earlier generation of effector cells to fight malignancy or infection, withheld effector function could assuage autoimmune cytotoxicity or prevent premature exhaustion of cells, and T cells that have become locked in a proliferative de-differentiated state may be pushed toward differentiation (Crompton, et al. 2014). When conceptualizing T cell differentiation and designing its experimental evaluation, it is important to uncouple differentiation and proliferation as two distinct processes that often coincide physiologically.

This body of work will describe the efforts to interrogate and control the differentiation process with methods which keep the proliferative abilities of the cell intact. As clinical data suggests that lesser-differentiated cells are more efficacious for tumour immunotherapy in addition to the aforementioned advantages of differentiation control (Gattinoni and Klebanoff, 2012), it is important to evaluate the therapeutic benefit in adoptive cell tumor therapy models of T cells with differentiation withheld through antibody-based and pharmacological means.

To begin, the ability of AKT inhibition to withhold differentiation of T cells during IL-2/TCR/CD28 stimulation was hypothesized and tested. This led to the observation of the uncoupling of the differentiation and proliferative processes of the cells by AKT inhibition (Leonardi and Crompton 2012, Crompton et al., 2015). Then the effectiveness of AKT inhibition in preventing differentiation and in allowing proliferation of stimulated human Tumor Infiltrating Lymphocytes (TILs) derived from resected melanomas was tested leading to the observation that T cells treated with AKT inhibitor demonstrated an *in vitro* advantage compared to cells that were untreated with AKT inhibitor (Crompton et al., 2015). The same study also investigated if withholding differentiation via AKT inhibition confers an *in vivo* cytotoxic, effector, and proliferative advantage to the cells in pre-clinical

models. These studies then seek to determine the tumor killing ability of cells treated with AKT inhibitor by treatment of mice bearing human tumors (xenograft model) and Murine tumors (syngeneic model) with adoptive transfer of tumor-specific T cells (Crompton et al., 2015, Klebanoff et al., 2017). Taken together the results demonstrated the pharmacological modulation of T cell differentiation was a possible option for additional TIL and Chimeric Antigen Receptor (CAR) clinical trials for the treatment of metastatic Melanoma.

With insight of the signalling mechanism of T cell differentiation through AKT, and the observation that antigen-experienced T cells cause accelerated (or precocious) differentiation of naïve T cells when exposed to one another, the hypothesis followed that there must be a communicable extracellular determinant of differentiation upstream of AKT by which Antigen-experienced cells cause the differentiation of their lesser-differentiated counterparts. To test this hypothesis of a paracrine model of differentiation, a method to track subsets of T cells with congenic markers *in vitro* and *in vivo* was designed in order to observe the phenotypes and function specific subsets had following stimulation (Klebanoff et al., 2016). Interrogating this hypothesis yielded experimental evidence demonstrating a paracrine, feed-forward mechanism of T-Cell differentiation caused by differentiated T cells expressing CD178/FasL (Klebanoff et al., 2016). In further development of this discovery, data reveals that T cells may be held in the stem cell memory and memory subsets during repeated stimulation by antibody blockade of CD178 (Klebanoff et al., 2016). Conversely, T cells in less differentiated subsets like naive and central memory may be pushed into effector status with exposure to leucine zipper FasL (lz-FasL) (Klebanoff et al., 2016). Given the clinical data describing how less-differentiated clonal populations of T cells are more likely to mediate tumor regression following adoptive transfer, the anti-tumor function of T cells treated with CD95L blocking antibody during stimulation and culture was tested in a syngeneic murine tumor treatment model. Indeed, their lesser-differentiated phenotype yielded a substantial benefit (Klebanoff et al., 2016).

Since the data revealed the profound effects of the CD95 and AKT signals on differentiation, this mechanistic insight could be applied to fields beyond tumor immunotherapy. Autoimmune Lymphocytic Proliferation Syndrome (ALPS) is a condition where patient's T cells have a CD95 signaling deficit due to a loss-of-function mutation,

which results in a proclivity for infection and Lymphoma (Cruz AC et al., 2016). Given a further understanding of T cell differentiation and as a credit to the discovery, collaborators hypothesized and verified the ability of T cells of ALPS patients to signal via AKT following CD95 stimulation along with their inability to apoptose (Cruz AC et al., 2016). Since ALPS patients have mutations in the CD95 domain that affect programmed cell death, or apoptosis, of T cells but not the differentiation of T cells, physicians and scientists can now appreciate the multifaceted role of CD95 in its cause of ALPS (Cruz et al., 2016). Furthermore, tumor immunity is not only dependent upon CD95/CD95L via differentiation of T cells, but also that collapse of the tumor stroma in T cell immunotherapies of cancer require CD95 stimulation on the stroma of the tumor itself, making CD95 a key therapeutic target in the tumor microenvironment (Kerkar et al., 2013).

This body of work updates the model of T cell differentiation from a nebulous confluence of cytokines and contexts, to a well-defined extracellular and intracellular signalling pathway that can be controlled for therapeutic benefit. The discovery of this mechanism and its ramifications for immunotherapy, infectious disease, and autoimmunity are discussed within this work, along with the methodology and experimental results of modulation of CD95 and AKT signaling within T cells.

2 LITERATURE REVIEW

2.1 Overview of Adoptive T-cell Therapy of Cancer

For decades, the treatment of cancer patients with T cells recognizing tumor-associated antigens had been practiced almost exclusively at the National Cancer Institute, but in the late 2000s, academic centers internationally began investigating this experimental, last-effort approach to fighting metastatic cancer (Radvanyi, 2015). Understandably, the therapy is not easily adopted due to the exceptional amount of individually-based steps involved which is the case for many such living therapies, but it offers great reward in unprecedented long-term response rates (Orlowski et al., 2017, Svane and Verdegall, 2014). As a barrier of entry to clinicians to employ use of Tumor Infiltrating Lymphocytes (TIL), there must be a skilled surgeon to remove a tumor in a patient, the tumor must be processed finely in a GMP laboratory, the T cells must be stimulated, cultured, and expanded to adequate numbers, the patient must be pre-conditioned by lymphodepleting chemotherapy prior to infusion, and post-infusion the patient must be critically monitored and treated for any immune-mediated reactions including shock, tumor lysis syndrome, cytokine release syndrome, autoimmunity, and pyrexia (Johnson and June, 2017).

An overview of the adoptive T-cell therapy process is shown in figure 1 (Leonardi and Modjtahedi, in preparation). Here, two separate paths of Adoptive cell Therapy are shown. The path to the left represents scenarios in which T cells must have a transduction in order to recognize the target antigen. These cells are taken from the peripheral blood of the patient or a matched donor, enriched, then transduced with a CAR or TCR, and stimulated in order to expand under varied conditions in order to optimize T cell function (Johnson and June, 2017). The path on the right represents the fragmenting of a tumor to extract the Tumor infiltrating lymphocytes, in which the tumor is processed via fragmentation, the T cells are stimulated and supported with cytokine and/or molecular agents, and sometimes transduced with specific proteins to maximize their tumor-killing efficacy (Hinrichs and Rosenberg, 2014). The cells can be divided into clones and selected for therapy based on cytotoxic protein release when exposed to the patient's tumor, or unselected (young TIL) and further expanded before being infused in the patient (Hinrichs and Rosenberg, 2014). The patient, represented by the figures in the center, is prepared for the infusion of cells by a myeloablative chemotherapy regimen of cyclophosphamide, fludarabine, or radiation

(Svane and Verdegall, 2014), (Wallen et al., 2009, Rosenberg et al., 2011). Cells are occasionally reinfused in cases where further tumor-killing is necessary and probable.

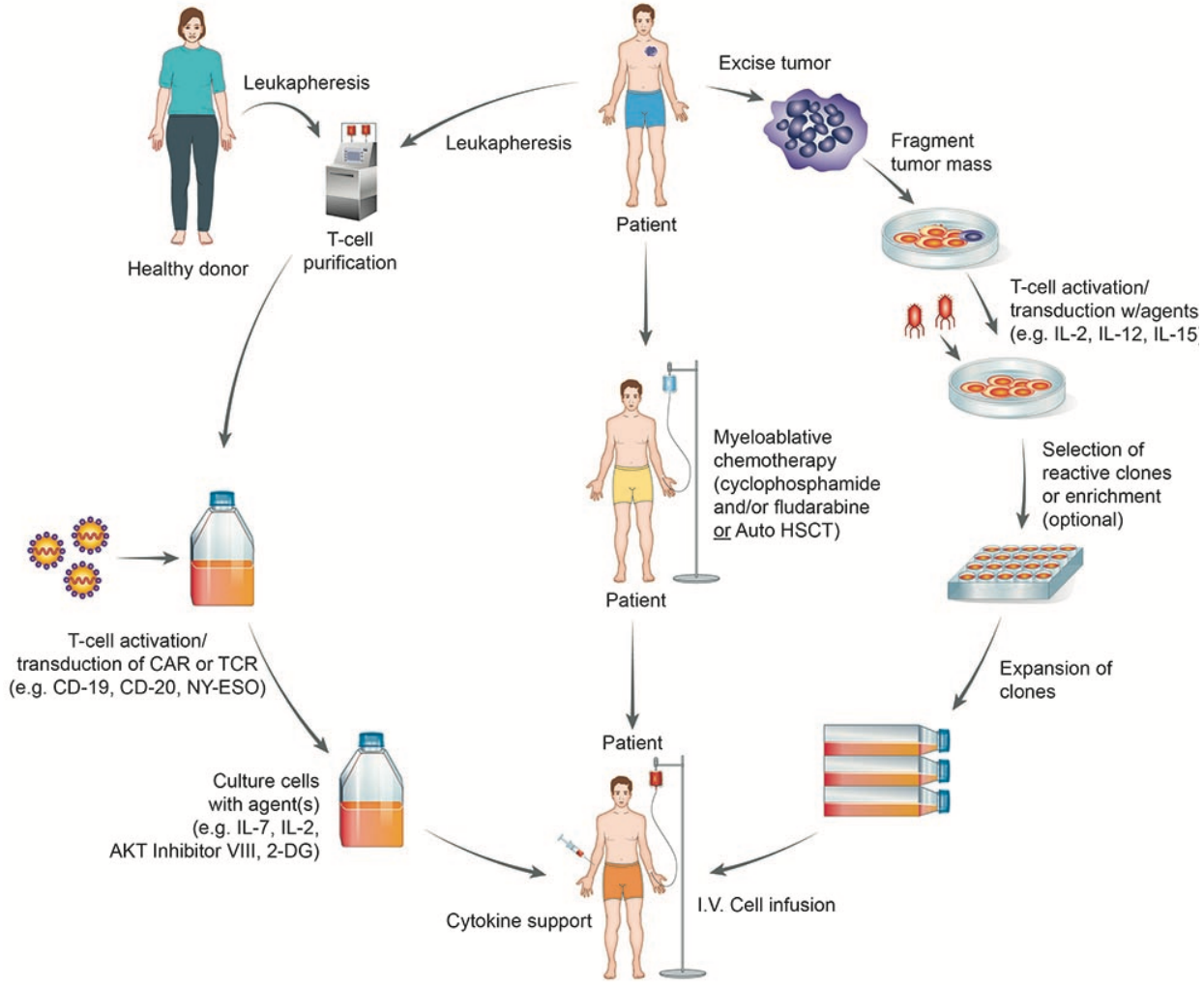

Figure 1 | Adoptive therapy process overview.
Two separate paths of Adoptive cell Therapy are shown. The path to the left represents scenarios in which T cells must have a transduction in order to recognize the target antigen. These cells are taken from the peripheral blood of the patient or a matched donor, enriched, then transduced with a CAR or TCR, and stimulated in order to expand under varied conditions in order to optimize T cell function. The path on the right represents the fragmenting of a tumor to extract the Tumor infiltrating lymphocytes, in which the tumor is processed via fragmentation, the T cells are stimulated and supported with cytokine and/or molecular agents, and sometimes transduced with specific proteins to maximize their tumor-killing efficacy. The cells can be selected based on this ability or unselected (young TIL) and further expanded before being infused in the patient. The patient, represented by the figures in the center, is prepared for the infusion of cells by a myeloablative chemotherapy regimen of cyclophosphamide, fludarabine, radiation, or a combination of these three. Cytokine support is given following infusion in the form of IL-2 injection. Cells are occasionally reinfused in cases where further tumor-killing is necessary and probable. (Leonardi and Modjtahedi, in preparation)

Adoptive immunotherapy of cancer was first used to treat patients in the late 1980s, with the use of tumor infiltrating lymphocytes in melanoma lesions resected from metastases (Rosenberg et al., 1988, Rosenberg et al., 2008). Figure 2 is a timeline outlining the development of tumor immunotherapy for two decades following the first use (Rosenberg et al., 2008).

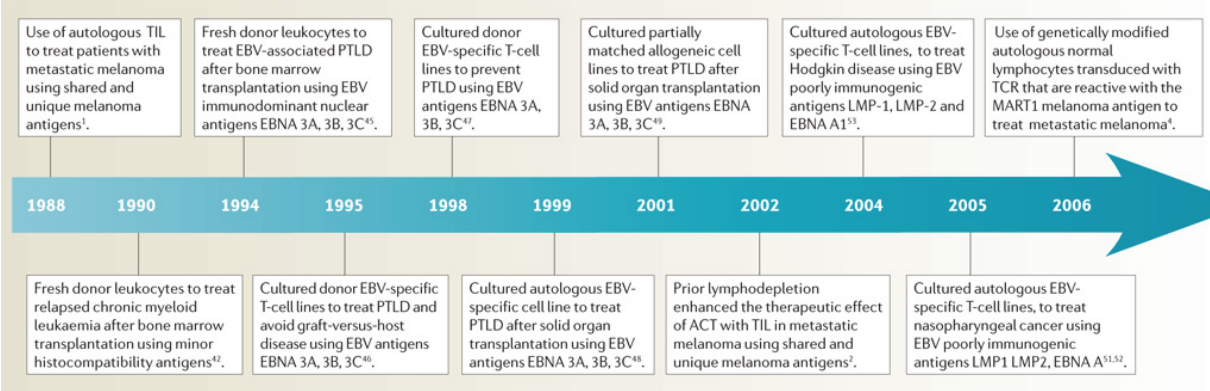

Figure 2 | Examples of ACT in patients with cancer EBV, Epstein–Barr virus; PTLD, post-transplant lymphoproliferative disease; TCR, T-cell receptor; TIL, tumour-infiltrating lymphocytes. Figure and Legend used with permission from Nature Reviews Cancer (Rosenberg et al., 2008).

Soon after the first use of TIL for melanoma, treatment of chronic myeloid Leukemia was attempted by transferring leukocytes harvested from donors matched in minor histocompatibility antigens in 1990 (Rosenberg et al., 2008, Kolb et al., 1990). All three patients had remissions of their cancer for 32-91 weeks following treatment (Rosenberg et al., 2008, Kolb et al., 1990). Attempts to treat additional histologies included use of donor T cell lines targeting Epstein Barr Virus associated Antigens for Hodgkin disease and Post Transplant Lymphoproliferative Disorder (PTLD) (Rosenberg et al., 2008, Rooney et al., 1998, Bollard C, et al., 2004). However, the T-cell receptors (TCRs) on these cells were naturally occurring. It was not until 2006 that lymphocytes were genetically engineered to express two distinct types of tumor antigen detecting proteins- one, a TCR much like those found endogenously on T cells, (Rosenberg et al., 2008, Morgan et al., 2006) and two, a chimeric antigen receptor (CAR), which is a protein chimera with an antibody-like extracellular domain and an intracellular T-cell CD3 signaling domain (Johnson and June, 2017, Dunn et al., 2004). More specifically, in the composition of a CAR, the heavy and light chains are linked by a Single-chain variable fragment and the same intracellular signalling domain as a T-cell, CD3, is used (Johnson and June, 2017). Figure 3 compares the CAR and the TCR (Johnson and June, 2017).

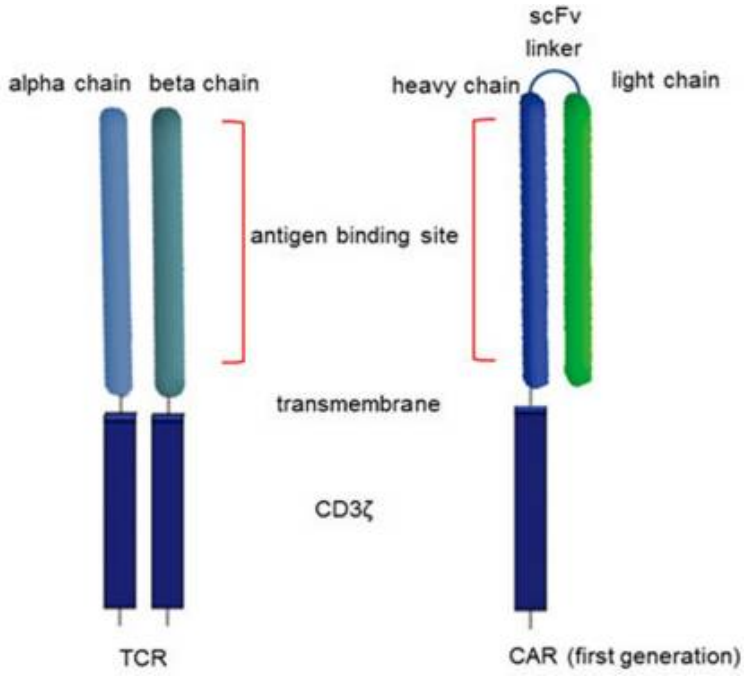

Figure 3 | T-cell receptor (TCR) and chimeric antigen receptor (CAR) structure. T-cell receptors are composed of two separate proteins, the alpha (α) and beta (β) chains. TCR antigen-binding sites are located in the membrane-distal variable regions, which are attached to the membrane-proximal constant region. CARs are composed of a membrane-distal single-chain variable region (scFv) made of the variable heavy and light chains joined by a linker molecule. Upon encountering cognate antigen, T-cell activation by both TCR and CAR occurs through intracellular TCR zeta (ζ) signaling. Figure and legend used with permission from Cell Research (Johnson and June, 2017).

2.2 Cancer Immunogenicity and the Tumor Microenvironment

The tumor microenvironment is a major factor contributing to the success of an adoptive cell transfer. Immune surveillance of cells exists in the steady state of an organism (Dunn et al., 2004). The adaptive immune system is capable of recognizing aberrant cellular facets such as genetic instability, in which cells proliferate into daughter cells which harbor heterogenous tumor-associated or tumor-specific cell surface markers (Dunn et al., 2004, Vinay et al., 2015). The genetic instability that creates markers for T cells to recognize can also create features which allow the tumor to evade the immune system (Dunn et al., 2004, Vinay et al., 2015). The quality of a tumor by virtue of this instability, to gain features which stimulate the immune response is known as immunogenicity. As stated earlier, tumors often contain T-cells (TILs) which recognize antigens expressed by the cancer. In these cases, the tumor is able to proliferate and evade destruction through several means, which constitute the concept known as immune evasion (Vinay et al., 2015). In tumor, myeloid cells which are responsible for antigen presentation may become dysfunctional

and no longer present antigen in a context which indicates need for destruction (Kerkar et al., 2011). In cases where the immune system surveils tissues and tumor, cooperation is necessary between Cytotoxic lymphocytes and myeloid-derived stromal cells, macrophages, and dendritic cells in which antigen is taken up and presented to CD8+ T cells in order to license the T cell to destroy tumor stroma in a mechanism known as cross-presentation (Kerkar et al., 2011). In a tumor's steady state, immune tolerance is induced and maintained by resident T-regulatory cells (Tregs) which are even more adept at quelling cytotoxic responses to tumor antigens than peripheral-blood resident Tregs (Chaudhary et al., 2016).

2.3 Factors Contributing to Successful Adoptive Immunotherapy of Cancer

In clinical and pre-clinical trials, decades of studies of ACT have been undertaken in order to discover and use the conditions that confer the best outcomes. With the observation of human clinical trials, correlates of successful tumor treatment can be uncovered. In addition to striking markers of a successful treatment like vitiligo one such correlate to success is the use of a lymphodepleting regimen prior to the infusion of the cancer-targeting T-cells (Rosenberg, et al., 2008). This is expected to be due to the aforementioned immune-suppressive environment which includes "cytokine sinks" (Gattinoni et al., 2005). These "cytokine sinks" are other immune cells such as T-regulatory cells which soak up the stimulatory cytokines like IL-2 and proliferate in the stead of the adoptively transferred cells (Gattinoni et al., 2005). In one clinical trial, the highest dose of total body irradiation given as a preparatory regimen at 1200cGy, correlated with the highest Objective Response Rate (ORR), presumably due to the ablation of "cytokine sinks" (Dudley et al., 2008). The dataset in this paper also revealed that higher levels of lymphodepletion also yielded higher concentrations of the lymphoproliferative cytokines IL-7 and IL-15 in serum, which are the cytokines that adoptively transferred T cells compete for with the cytokine sinks (Dudley et al., 2008). In further analysis of T cell phenotypic correlates to tumor response, the identification of factors deemed beneficial by virtue of more youthful T cells was made, as indicated by longer telomeres, higher expression of CD27 (which is a TNF family receptor necessary for the maintenance of memory) (Hendriks et al., 2000), and longer *in vivo* persistence (Rosenberg et al., 2011).

This data reaffirmed the necessity of the efforts to elucidate the mechanisms of T-cell persistence, especially for the use of adoptive cell therapies. Additionally, many pre-clinical models have shown that the differentiation status of cells correlates with their *in vivo* efficacy in adoptive immunotherapy of cancer. In the following section, the differentiation of T-cells will be discussed from naive to effector with emphasis on the application to adoptive cell therapies.

2.4 T-cell Differentiation

Like many other tissues in the body including the central nervous system, the intestines, skin, lungs, and heart, lymphocytes also have stem cells which are marked by the ability to self-renew and divide asymmetrically (Klebanoff and Gattinoni, 2012). After division, the daughter cells may undergo differentiation into subsets which are prompted contextually by antigen presenting cells (APCs) (Klebanoff and Gattinoni, 2012). These subsets follow a progressive model of differentiation from the Naive state, in which the cell has not been stimulated to a final state of effector, as evidenced by the epigenetic landscape and ability of the cells to self-renew in transplant experiments (Crompton et al. 2016). Figure 4 details the differentiation states of a T-cell and the markers associated with each stage along the lifespan of a T cell (Klebanoff and Gattinoni, 2012).

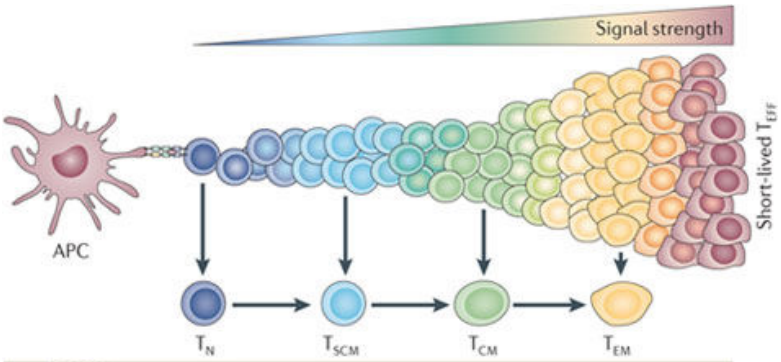

		T_N	T_{SCM}	T_{CM}	T_{EM}
Phenotype	CCR7	+++	+++	++	–
	CD62L	+++	+++	++	–
	CD27	+++	+++	++	+/–
	CD28	++	+++	+++	+/–
	CD45RA	+	+	–	+/–
	CD45RO	–	–	+	+
	CD122	–	++	+++	+++
	CD95	–	++	+++	+++
	KLRG1	–	–	+/–	++
Transcription factors	TCF7	+++	+++	++	+
	ID3	+++	+++	++	+
	LEF1	+++	++	+	–
	FOXP1	+++	++	+	–
	KLF7	+++	++	+	–
	EOMES	+	+	+	++
	ID2	+	+	++	+++
	PRDM1	–	+	+	+++
	TBX21	–	+	++	+++
	ZEB2	–	+	++	+++
miRNA	let7 family	+++	ND	ND	–
	miR-26a/b	+++	ND	ND	–
	miR-29a/b	+++	ND	ND	–
	miR-30a-5P	+++	ND	ND	–
	miR-142-5P	+++	ND	ND	+++
	miR-21	–	ND	ND	+++
	miR-146	–	ND	ND	+++
	miR-155	–	ND	ND	+++
Function	IFNγ	–	+	++	+++
	IL-2	–	++	+++	+/–
	Cytoxicity	–	+/–	+	+++
	Telomere	+++	+++	++	+
	Self-renewal	+	+++	++	+

Nature Reviews | Cancer

Figure 4 | A model of progressive T cell differentiation. During an immune response, naive T (TN) cells are primed by antigen-presenting cells (APCs). Depending on the strength and quality of stimulatory signals, proliferating T cells progress along a differentiation pathway that culminates in the generation of terminally differentiated short-lived effector T (TEFF) cells. When antigenic and inflammatory stimuli cease, primed T cells become quiescent and enter into the memory stem cell (TSCM), central memory (TCM) cell or effector memory (TEM) cell pools depending on the signal strength received. The phenotypic attributes, expression levels of key transcription factors and

Figure 4… microRNAs (miRNAs), and the functional properties of naive and memory T cell subsets are illustrated as not expressed (–), low expression (+), intermediate expression (++) and high expression (+++). EOMES, eomesodermin; FOXP1, Forkhead box P1; ID, inhibitor of DNA-binding; IFNγ, interferon-γ; IL-2, interleukin-2; KLF, Kruppel-like factor; KLRG1, killer cell lectin-like receptor subfamily G, member 1; LEF1, lymphoid enhancer-binding factor 1; ND, not determined; PRDM1, PR domain-containing 1 with ZNF domain; TBX21, T-box 21; TCF7, T cell factor 7; ZEB2, zinc finger E-box binding homeobox 2. Figure and Legend used with permission from Nature Reviews Cancer. (Klebanoff and Gattinoni 2012).

When T cells are adoptively transferred in order to target a tumor, their differentiation state must best considered in order to confer the best chances of mediating tumor regression (Klebanoff and Gattinoni, 2012). In cases where lesser differentiated cells are used to target tumor, there will be greater proliferative capacity and ability to remain in the patient, but when a more effector-type population is used, these cells will lack proliferative capability and the ability to travel to the lymph nodes and meet with resident antigen presenting cells (Klebanoff and Gattinoni, 2012). Figure 5 illustrates the scenarios of Adoptive transfer of T cells in different differentiation states for the treatment of tumor (Klebanoff and Gattinoni, 2012).

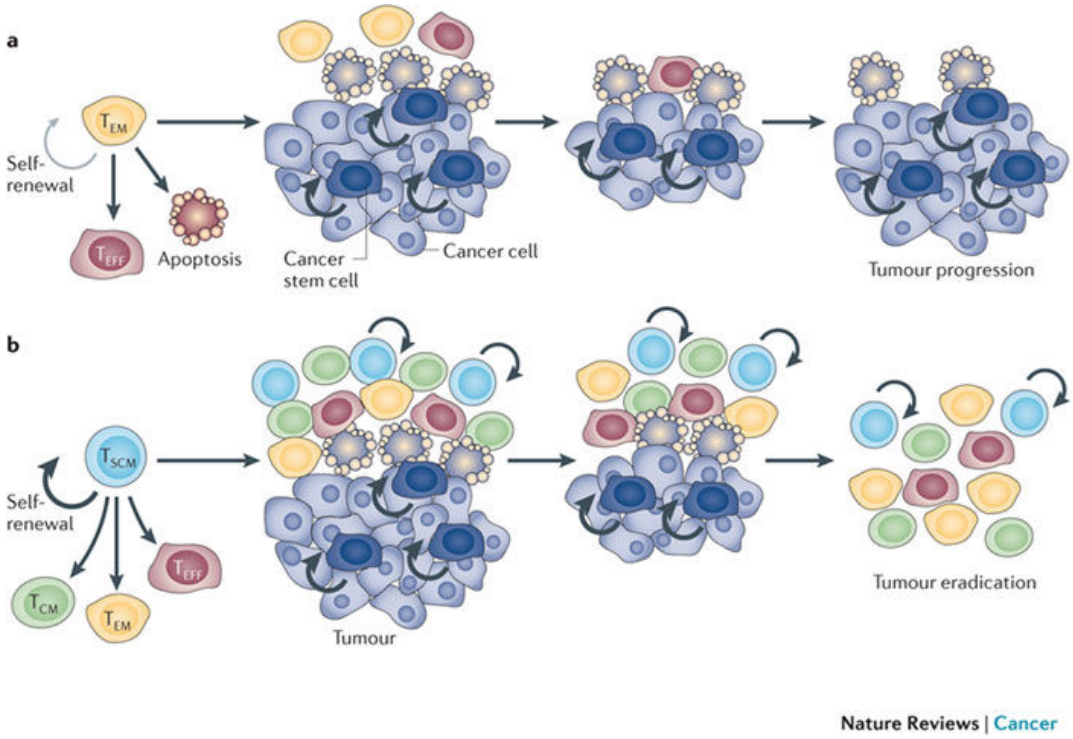

Figure 5 | Fighting fire with fire. A | Current T cell based immunotherapies predominantly transfer cells with effector memory (TEM)-like phenotypic and functional characteristics. These cells have limited self-renewal capacity and are oligopotent. These cells can mediate tumour destruction but are handicapped to compete with expanding tumor masses (shown as purple tumour cells) that are sustained by the activity of self-renewing multipotent cancer stem cells (CSCs; shown as dark purple tumour cells). B | Future T cell-based immunotherapies might benefit from the transfer of T memory stem cells (TSCM) that have enhanced self-renewal and the multipotent capacity to form all memory and effector subsets. These properties allow TSCM cells to sustain a prolonged immune attack by giving rise to more differentiated, highly lytic effector T (TEFF) and TEM cells while maintaining a continuous supply of less differentiated TSCM and central memory (TCM) cells that can refresh the pool of cytotoxic T cells over time. In this manner, TSCM cells might overtake the last tumour cell, including CSCs, and so cure the host. Figure and legend used with permission from Nature Reviews Cancer (Klebanoff and Gattinoni, 2012).

Given the biology of T cells in which they are limited in their ability to proliferate and self-renew, a reasonable goal in the field of adoptive T cell immunotherapy is control of T cell differentiation states in order to withhold premature effector differentiation (Klebanoff and Gattinoni, 2012). Control of differentiation is not the only facet of T-cell function, metabolism is also an integral component of a cell which would dictate its duration of life and persistence (Sukumar et al., 2013). The relation of T cell metabolism to tumor immunotherapy will be briefly discussed in the following section.

2.5 T cell Metabolism

Metabolic function of cells is tightly correlated with differentiation state and function, with naive cells exhibiting fatty acid oxidation and effector cells exhibiting anaerobic glycolysis (van der Windt and Pearce, 2012). Notably in 2011, it was found that the AKT signalling protein was dispensible for T-cell proliferation, and that AKT inhibition did not hinder IL-2 driven glycolytic function (van der Windt and Pearce, 2012, Macintyre et al., 2011). Furthermore, the treatment of cells with AKT inhibitor maintained a greater level of expression of the memory-associated lymphoid homing marker CD62L compared to stimulation without the inhibitor (Macintyre et al., 2011). This data supported the idea that differentiation could be uncoupled from proliferation.

2.6 Strategies Targeting T-Cell Function to Optimize Adoptive T-Cell Therapy of Cancer

In order to maximize the effectiveness of adoptive cell therapy, T cells must be selected and fine-tuned for the process, culminating in the maintenance of a T cell population that will recognize and kill cells bearing tumor-associated antigen (Klebanoff and Gattinoni, 2012). The response of a T cell to antigen depends upon a gamut of contexts, and is a diverse and complex field of study. Equally complex are the variables to what makes a persistent, self-renewing population of anti-cancer T cells. Harnessing particular physiological (and if achievable, extra-physiological) states of T cell function by manipulation of contextual signalling proteins (both natural and artificial e.g. CARs) and substrates to achieve a response to tumor is the predominant goal in adoptive T-Cell Immunotherapy.

The current strategies of enhancing the efficacy of Adoptive Tumor Immunotherapy by methods believed to augment the tumor killing response of T-cells focus on different aspects of cell biology. These include but are not limited to: targeting cell metabolism, targeting intracellular cell signaling, checkpoint blockade, altering T-cell fate or differentiation, and stimulation the T cells with certain contextual proteins or cytokines. It must be noted, however, that any particular strategy of intervention does not exert an effect merely on that particular system, but will yield effects detectable on other physiological

systems of the T cell (Sukumar et al., 2013). For example, a metabolic strategy of altering T cell function may yield an effect seen on the differentiation of the cell, and vice-versa (Sukumar et al., 2013). The uncoupling of given physiological systems (e.g. differentiation, metabolic, cell-fate, proliferation) can be seen with particular strategies (between differentiation and proliferation, for example, as is the case in AKT inhibition), but the metabolic and proteomic signatures of the cell remain coherent following intervention upon a particular system when measuring the qualities of other systems of the cell (Crompton et al., 2015, Sukumar et al., 2013, Sukumar and Gattinoni 2014, Sukumar et al., 2016). This section will briefly mention the efforts to better T-cell function for adoptive immunotherapy of cancer in order to create context for the efforts described in the results.

2.6.1 Optimization of Therapies Using a Chimeric Antigen Receptor

CARs have undergone continuous development and optimization, with new iterations termed “generations” (Johnson and June 2017). Selected methods to optimize CAR therapy are summarized in Table 1 (Leonardi and Modjtahedi, in preparation). Some of these methods may include additional costimulation to the first generation CAR (Finney, et al., 1998, Weigelin, et al., 2016, Hombach & Abken, 2013, Zhong, et al., 2010), strategies to enrich for CAR T-cells prior to infusion which are more likely to function optimally (Chang, et al., 2015, ClinicalTrials.gov Identifier: NCT02652910), a method for creating CAR-T cells which can be grafted into any person (universal CAR) (Qasim, et al., 2017), and methods to construct the CAR’s moieties for optimal targeting and function (Watanabe, et al., 2016, Osborn, et al., 2016).

Method	Agent	Method of Action	Execution	Reference
CD25+ CAR^{hi}	Protein	Selection	FACS Sort	Chang, et al., 2015
CD-28 Costimulatory Domain (2^{nd} gen CAR)	Protein	Activation/ Costimulation	Viral Construct	Finney, et al., 1998.
4-1BB Costimulatory Domain (2^{nd} gen CAR)	Protein	Activation/ Costimulation	Viral Construct	Weigelin, et al., 2016
CD-28 & 4-1BB Costimulatory Domains (3^{rd} gen CAR)	Protein	Activation/ Costimulation	Viral Construct	Zhong, et al., 2010
OX-40	Protein	Activation/ Costimulation	Viral Construct	Hombach & Abken, 2013
Spacer Domain Modification (CH3 only)	Protein	Controlled Tonic Signalling	Viral Construct	Watanabe, et al., 2016.
CAR Knock-in/TCR Knock-out	Protein	Expression	CRISPR/Cas9	Osborn, et al., 2016
AB TCR & CD52 Deletion (Universal CAR T-Cells)	Protein	Controlled Cell Activation/Specificity	TALEN	Qasim, et al., 2017
Memory-enriched CAR (meCAR)	Protein	Selection	Cell Sort	NCT02652910

Table 1 | CAR Optimization. Selected strategies to optimize the function and tumor responses of CAR-T therapies which target the T-cell are shown above. (Leonardi and Modjtahedi, in preparation)

2.6.2 Strategies Which Target the Metabolism of T Cells

Targeting cellular metabolism in adoptive immunotherapy is a relatively novel approach, with recent studies showing T cells ramp up their energy expenditure and glucose uptake from memory to effector, and that the formation of memory and long-lived cells can be achieved with Fatty acid oxidation (FAO) instead of glycolysis (Sukumar and Gattinoni, 2013, Pearce, et al., 2009). On the basis of this insight, further development has shown that T cells stimulated in the presence of the glucose uptake inhibitor 2-DG were shown to possess enhanced memory and antitumor function (Sukumar et al., 2013). While it could be metabolically reprogramming cells from high glucose consumption to low, it could also

be selecting out high glucose consuming cells and yielding a less glycolytic population for infusion.

2.6.3 Strategies Which Target Contextual Signaling of T Cells

The control of T-cell activity and function can be achieved by use of cytokines. These are proteins which are secreted by cells that affect the behavior of other cells, and are used to provide contextual signals. For example, the cytokine IL-2 secreted predominantly by CD4+ T-cells and causes proliferation and glycolysis of CD8+ T cells and other cells which it signals upon (Klebanoff et al., 2004). This section will briefly describe some of the important cytokines for optimizing T cell function in adoptive immunotherapy of cancer.

IL-2. During the *in vitro* T-cell stimulation and expansion phases the viability of the T-cells depends upon IL-2 much like glucose and serum are necessary for any culture. In fact, IL-2 provides a context which causes the T cell to execute a program which includes the very consumption of glucose and division of the cell (Boyman and Sprent, 2012). The feedback between physiological systems of a cell is evident by virtue of metabolic changes, differentiation states, cell proliferation, and gene expression data with the addition of IL-2 to a T cell culture. Indeed, increased levels of IL-2 can supplement a weak or non-existent CD-28 signal and enact these programmatic changes (Frauwirth et al., 2002). In addition to its role in the maintenance of T cell culture, IL-2 is given to patients following the adoptive transfer of T-cells (Radvanyi, 2015). For the foreseeable future IL-2 will keep its role as a mainstay in the maintenance of T cell cultures and their preparation for Adoptive Cell Transfer.

IL-7. Evidence supports a role of IL-7Rα expression on mouse T cells enabling the engraftment of cells transferred in mice in vivo (Johnson et al., 2016). In a depletion model, the absence of host-provided IL-7 caused severely impaired persistence compared to controls. Furthermore, cells deficient in IL-7Rα expression phenocopied Wild-type (WT) T-cells in vitro but had engraftment difficulties similar to the experiment in which the host was depleted of IL-7. This suggests that the maintenance of IL-7 signaling following the transfer of cells may be a point of intervention, perhaps even to the point of achieving supraphysiological levels.

IL-12. The Ex-vivo priming of T cell cultures with IL-12 has shown to yield an advantage in tumor immunotherapy (Rubinstein et al., 2012), as has its forced expression in T cells prepared for transfer, which continually express IL-12 (Kerkar et al., 2013, Lasek and Zagozdzon, 2016). Both of these strategies have impressive pre-clinical data with the latter having clinical trials, which were halted due to excessive host immune response (Lasek et al., 2014).

IL-15. The effects of IL-15 on cell metabolism and differentiation appear promising when examined at many points on the path of Adoptive Cell Transfer. The cytokine has shown to promote T cell expansion when infused in vivo (Sneller et al., 2011) and memory formation when provided in vitro; in pre-clinical models of adoptive cell immunotherapy, T cells cultured in IL-15 have shown superior anti-tumor efficacy when compared to IL-2 (Klebanoff et al., 2004).

IL-33. IL-33 is a potent cytokine which can slow growth of tumors when provided exogenously through CD8+ T cell mediated tumor killing (Dominguez et al., 2017). In a mouse lymphoma model IL-33 has also been shown to stimulate the growth of human Vγ9Vδ2 T cells that can prevent tumor growth after adoptive transfer (Duault et al., 2017).

POTASSIUM MODULATION. Extracellular potassium was shown to withhold effector differentiation in the tumor microenvironment- an effect abrogated with the enforced expression of Kcna3, a potassium inporter (Eil et al., 2017). This is beneficial for the prevention of premature effector function, which would result in poorer tumor treatment.

TNF BLOCKADE. TNFa knockout T-cells adoptively transferred into tumor-bearing mice have been shown to yield superior antitumor efficacy compared to controls, believed to be due to in part by the effect on tumor neovascularization (Alam, et al., 2015). It has been proposed that blockade of TNFR2 may target TNFR2+ tumor-infiltrating Tregs and allow for the killing of TNFR2-expressing tumors.

USE OF ALL-TRANS RETINOIC ACID (ATRA). In a pre-clinical model of adoptive immunotherapy with CD4+ T cells, groups of mice receiving ATRA survived longer compared to controls, due to a significant difference in tumor treatment (Klebanoff et al.,

2013). Mechanistic inquiry in the study revealed that ATRA treatment forced the endogenous Dendritic cell progenitors into a CD11b+CD8α− lineage, which directly stimulated the adoptively transferred CD4+ T-cells. In the absence of ATRA, CD4+ T cells did not have a sufficient population of CD11b+CD8α− dendritic cells for their stimulation, instead a population of CD11b+CD8α+ dendritic cells took hold, meaning in cases where CD4+ T cells are adoptively transferred, the lineage of dendritic cells should be controlled for optimal responses (Klebanoff et al., 2013).

2.6.4 Strategies Targeting Intracellular Cell Signaling of T Cells

With the use of pharmacological and other agents which target the intracellular machinery of cells, cell surface proteins may be bypassed and certain pathways may be targeted. This section will briefly detail such methods that have been employed to better T cells for adoptive immunotherapy.

In a mouse adoptive immunotherapy model, *in vitro* stimulation with a PI3K inhibitor conditioned T cells to better treat tumor than controls in a mouse adoptive immunotherapy model (Eid et al., 2017). The cells were presumed to be superior due to their enhanced proliferative ability and memory phenotype. In another study which targeted HIF-Hydroxylase with the agent dimethyloxalylglycine (DMOG), CD4+ TRP-1 splenocytes treated with DMOG during stimulation treated tumor significantly better than controls, presumably due to the increased population of cells committing to the Th1 lineage over the Treg lineage (Clever et al., 2016). In different terms, treatment of these CD4+ T cells with DMOG pushed their differentiation into effector cells which lyse tumor instead of T regulatory cells which would dampen the tumor response. This differs from the human experience, however, in that splenocytes which are CD4+ Th1 progenitors are not acquired for human immunotherapy, but rather T cells which have already differentiated away from the T regulatory fate are excised and used as TIL (Gattinoni et al, 2012).

Targeting the mammalian Target of Rapamycin (mTOR) has also been used for conditioning T cells during adoptive immunotherapy. Treatment of mice with rapamycin in vivo enhanced the effector and memory CD8+ T cell function induced by Ad-Flt3L + Ad-TK/GCV and increased therapeutic efficacy in an adoptive cell therapy mouse model of glioma (Mineharu et al., 2014).

2.6.5 Strategies Targeting Checkpoint Inhibitors of T Cells

Since 1975, a wide range of antibodies have been approved which either target tumor antigen, or target immune checkpoint inhibitors. These checkpoint inhibitors are proteins on the T cell surface that block or inhibit T cell function when they are stimulated (Fig. 6, Drew Pardoll, 2012). In one notable example, Pembrolizumab, an antibody targeting programmed cell death protein 1 (PD1), was FDA approved for individuals with microsatellite instability–high (MSI-H) or mismatch-repair–deficient (dMMR) solid tumors (Lemery, et al., 2017). Antibodies against checkpoint inhibitors work by blocking the inhibitory interaction between ligands on tumor and receptors on T-cells, and thereby allow the T cells to function (Lemery, et al., 2017). Checkpoint inhibitor blocking antibodies have been found to enable T cell escape from anergy *in vitro* as well as *in vivo*, and when used in combination with adoptive cell therapy (Serganova, et al., 2017). This section will discuss some of the strategies for improving adoptive immunotherapy by use of these checkpoint inhibitors in combination.

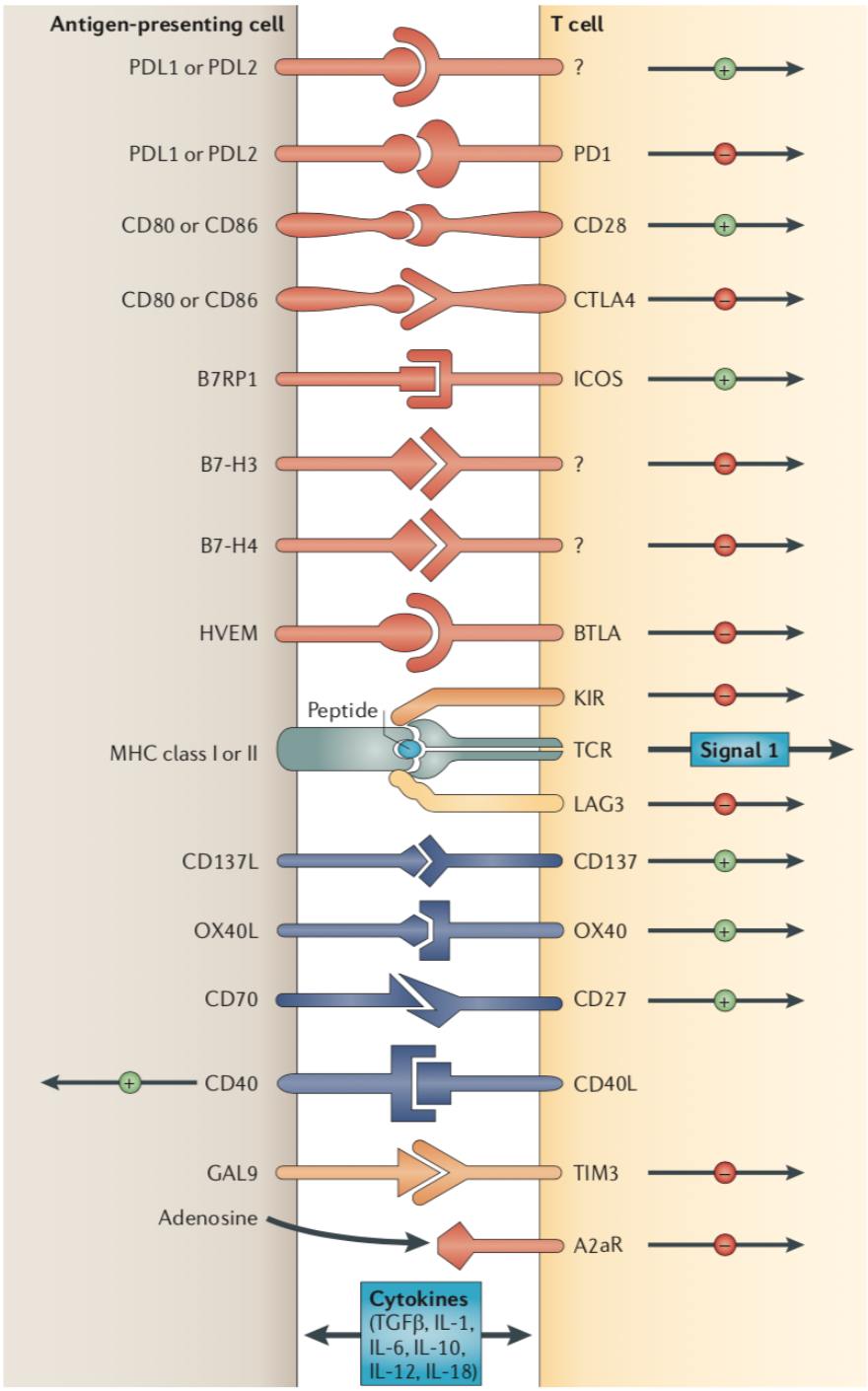

Figure 6 | Multiple co-stimulatory and inhibitory interactions regulate T cell responses. Depicted are various ligand–receptor interactions between T cells and antigen-presenting cells (APCs) that regulate the T cell response to antigen (which is mediated by peptide– major histocompatibility complex (MHC) molecule complexes that are recognized by the T cell receptor (TCR)). These responses can occur at the initiation of T cell responses in lymph nodes (where the major APCs are dendritic cells) or in peripheral tissues or tumours (where effector responses are regulated). In general, T cells do not respond to these ligand–receptor interactions unless they first recognize their cognate antigen through the TCR. Many of the ligands bind to multiple receptors, some of which deliver co- stimulatory signals and others deliver inhibitory signals. In general, pairs of co-stimulatory–inhibitory receptors that bind the same ligand or ligands — such as CD28 and cytotoxic T-lymphocyte-associated antigen 4 (CTLA4) — display distinct kinetics of expression with the co-stimulatory receptor expressed on naive and resting T cells, but the inhibitory receptor

Figure 6… is commonly upregulated after T cell activation. One important family of membrane bound ligands that bind both co-stimulatory and inhibitory receptors is the B7 family. All of the B7 family members and their known ligands belong to the immunoglobulin superfamily. Many of the receptors for more recently identified B7 family members have not yet been identified. Tumour necrosis factor (TNF) family members that bind to cognate TNF receptor family molecules represent a second family of regulatory ligand–receptor pairs. These receptors predominantly deliver co-stimulatory signals when engaged by their cognate ligands. Another major category of signals that regulate the activation of T cells comes from soluble cytokines in the microenvironment. Communication between T cells and APCs is bidirectional. In some cases, this occurs when ligands themselves signal to the APC. In other cases, activated T cells upregulate ligands, such as CD40L, that engage cognate receptors on APCs. A2aR, adenosine A2a receptor; B7RP1, B7-related protein 1; BTLA, B and T lymphocyte attenuator; GAL9, galectin 9; HVEM, herpesvirus entry mediator; ICOS, inducible T cell co-stimulator; IL, interleukin; KIR, killer cell immunoglobulin- like receptor; LAG3, lymphocyte activation gene 3: PD1, programmed cell death protein 1; PDL, PD1 ligand; TGFβ, transforming growth factor-β; TIM3, T cell membrane protein 3. Figure and legend used with permission from Nature Reviews Cancer (Drew Pardoll, 2012).

CTLA-4 BLOCKADE. Strategies combining the agents targeting checkpoint inhibitors and adoptive immunotherapies have recently emerged to success. In a mouse model of ACT where anti-CTLA-4 blocking antibody was infused in vivo alongside the transferred cells, the group with the combined therapy exhibited an additive effect (Mahvi, et al., 2015). There is an ongoing clinical trial using this strategy to target Uveal melanoma at the M.D. Anderson Cancer Center (ClinicalTrials.gov Identifier: NCT03068624).

OX40 STIMULATION. Data has shown that OX40 stimulation combined with CD28 stimulation on CAR-T Cells can reactivate cells residing in peripheral tissues (Hombach & Abken, 2013). However, the same group to show this later presented CD28 stimulation alone as superior in CAR-transduced Cytokine Induced Killer Cells, given the propensity for the combination of CD28 and OX40 to induce Activation Induced Cell Death (AICD) (Hombach, Rappl, & Abken, 2013). The cells with combined OX40 signal were shown to yield lower antitumor efficacy in vivo.

PD-1/PD-L1 BLOCKADE. Modulation of the PD-1/PD-L1 axis has been widely successful as a monotherapy of cancer. With consideration of the mechanism of action and the effect of the protein's inhibition on T-cells, recent studies have shown that in vivo antagonization of PD-1/PD-L1 with Adoptive Cell Transfer of CAR-T cells yields better antitumor efficacy than cells alone (Serganova, et al., 2017).

4-1BB STIMULATION. A combined approach of tumor therapy of CD137 agonization and adoptive immunotherapy seems an enticing option (Weigelin, et al., 2016). A recent

clinical trial has shown that agonization of CD137 synergizes with adoptive cell transfer in the treatment of cancer in a trial of EBV positive tumors (Eom, et al., 2016).

2.6.6 Strategies Targeting Cell Differentiation

Another strategy for improving adoptive immunotherapy would be to control the differentiation state of the T cells directly. By reprogramming the T cells with transcription factors associated with the subset desired or into induced pluripotent stem cells (IPSCs), younger and more proliferative T cells may be used for adoptive immunotherapy (Vizcardo et al., 2018). This technique is more difficult than traditional methods, however, in that the efficiency in reprogramming makes for the isolation in relatively few clones (Vizcardo et al., 2018). Furthermore, in cases where T cell populations may be selected from blood for use of adoptive immunotherapy such as CAR-T or TCR immunotherapies, there may be sufficient numbers of lesser-differentiated cells to choose from (Turtle, et al., 2011, Riddell et al., 2014).

2.7 Current Challenges in the Field

Despite the advances in adoptive immunotherapy two important challenges in the field remain: treating the toxicity associated with the T cell response, and using less-differentiated, more proliferative cells for adoptive transfer. This section will highlight these challenges.

Both clinical and pre-clinical data show T cell differentiation state as a major factor in treatment efficacy. As described by Klebanoff and Gattinoni, the use of effector populations of cells rather than memory will not enable cancer-targeting T-cells to self-renew and fill the memory compartments (Klebanoff and Gattinoni, 2012). Additionally, by use of new technology enabling the tracking of specific populations of T-cell clones after infusion, tumor responses have been correlated with lesser-differentiated clones rather than their more-differentiated counterparts (Watkins and Miles, 2017). Therefore, in order to optimize cell therapy and create more durable responses in patients, controlling the T cell differentiation state is a prime goal. This is a challenge however, in that during stimulation of T cells *in vitro* in order to condition them for cytotoxic response to tumor

and multiply them in adequate numbers prior to transfer, they differentiate while proliferating (Crompton et al., 2014). Therefore there is a need to uncouple differentiation from proliferation (Crompton et al., 2014).

While the benefits and capabilities of employing the immune system with adoptive cell therapies are numerous, efforts to rectify the associated toxicities must be made. In the goal of creating T cells which adequately respond to tumor there is a fine line where therapies that may be too strong for the patient begin (Lasek and Zagozdzon, 2016). The consideration of how potent an effector response needs to be must be balanced with the possibility of toxicity for the patient. Toxicities associated with adoptive transfer of T cells for the treatment of cancer include cytokine release syndrome (CRS), tumor lysis syndrome, shock, pyrexia, neuroedema, and lung failure (Neelapu et al., 2018). The prevalence of such toxic events is seen as high as 13 percent of the time for CRS and 28 percent of the time for neurological toxicities (Neelapu et al., 2018). In the vast majority of cases, a critical care center familiar with treating patients who have undergone adoptive immunotherapy is able to treat these events, which typically are of limited duration. In fact, clinicians familiar with treating leukemia patients with CD19 CARs recognize the severity of CRS to correlate with the degree of anti-tumor response (Johnson and June, 2017, Davila et al., 2014) Additionally, seemingly safe antigens to target with CARs may prove to be hazardous due to the potency of the therapy, which was an issue with a CAR recognizing the antigen HER2 (Johnson and June, 2017). In this case, the first patient on the trial was infused with with $1 \text{ X } 10^{11}$ T-cells and immediately went into shock, coma, and died 5 days later, despite full medical intervention. Expression of HER2 on lung epithelium was found to be the cause of the toxicity, even though such toxicity is not seen with the HER2 antibody the CAR was designed after (Johnson and June, 2017). Therefore, if there is to be wide approval and adoption of cell therapies for cancer, there must be further investigation of possible toxicities and their managements must be perfected and widely known, or such toxicity abrogated altogether.

3 HYPOTHESES TO BE ADDRESSED BY THE WORK

Based on a prior study showing that the presence of antigen experienced cells brings up the differentiation baseline of the cell culture in total (Hinrichs et al., 2011) there is evidence to hypothesize a paracrine mechanism for T-cell differentiation. Such a mechanism would represent a contextual, or extracellular signal. In consideration of this, given the expression profile of the Fas receptor in which it is upregulated on stem cell T cells (Gattinoni et al., 2011) signaling through the Fas receptor is a viable candidate for a paracrine mechanism of differentiation. As the efficacy of T cell adoptive immunotherapy of cancer is correlated with T cell differentiation, the ability to further control and withhold differentiation of the cells may increase treatment efficacy (Klebanoff and Gattinoni, 2012).

To follow the differentiation signal to a point of intracellular signal transduction, based on data showing that AKT signaling is not necessary for cell proliferation and that inhibition of AKT causes the retention of CD62L, it is reasonable to hypothesize differentiation and proliferation have been uncoupled, and that the cell differentiation signal propagates through AKT (Macintyre et al., 2011). Given the lesser differentiated phenotype of the cells treated with AKT inhibitor, there may be a benefit to cell therapy uses including adoptive immunotherapy (Macintyre et al., 2011, Hinrichs et al., 2011).

4 AUTHOR'S PUBLISHED DATA AND CONCLUSIONS

This section will highlight key figures from the author's publications which address the hypotheses. All published work represented in the figures is referenced along with the specific methods published by the author. The purpose of this section is to present a narrative detailing the discoveries that highlights the contributions of the author to the field.

4.1 Nonapoptotic Fas Signaling Causes T Cell Differentiation

In order to investigate the possibility of a Fas/CD95 mediated effect on CD8+ T-cell differentiation, murine CD8+ naive T cells were purified through negative selection and stimulated with increasing amounts of recombinant human FasL (leucine zipper FasL or lz-FasL) maintained in culture for 6 days (methods 7.1, 7.2, 7.8, and 7.9). After 6 days in culture the differentiation state of these cells was analyzed by flow cytometry (methods 7.3 and 7.13) (Fig 7 A, B), with restimulation and intracellular staining performed in order to characterize interferon gamma release, which is a marker for effector capability.

Given that this phenomenon could be explained by the selective deletion/apoptosis of naive and central memory cells in culture, suggested by the progressively lower cell yields with increased levels of lz-FasL (method 7.2) (Figure 7 C, D), the following experiment utilized two murine transgenic models of Fas loss of function (method 7.4). Lpr mice have no functional Fas receptor present, and C194V mice have a single mutation at the 194 site of Fas from Valine to Cysteine, which is published to nullify the apoptotic signal. If the hypothesis that a non-apoptotic signal conferred by Fas stimulation causes T-cell differentiation is correct, then treatment of C194V T cells may exhibit the differentiation phenotype but not the lpr T cells. If the lpr T cells revealed an effect, it would exist outside of the Fas signal. If there was not an effect in the C194V T cells, then the effect may be mediated along with the apoptotic signal.

To analyze the effect of lz-FasL on cell death in these cells, CD8+ T cells were incubated for 6-8 hours with specified levels of lz-FasL and analyzed for PI and annexin positivity by flow cytometry (methods 7.3 and 7.9) (Figure 7 E). Following stimulation and culture for 6

days with and without Fas-lz, the differentiation states of the three strains were analyzed by flow cytometry and compared (methods 7.3) (Figure 7F).

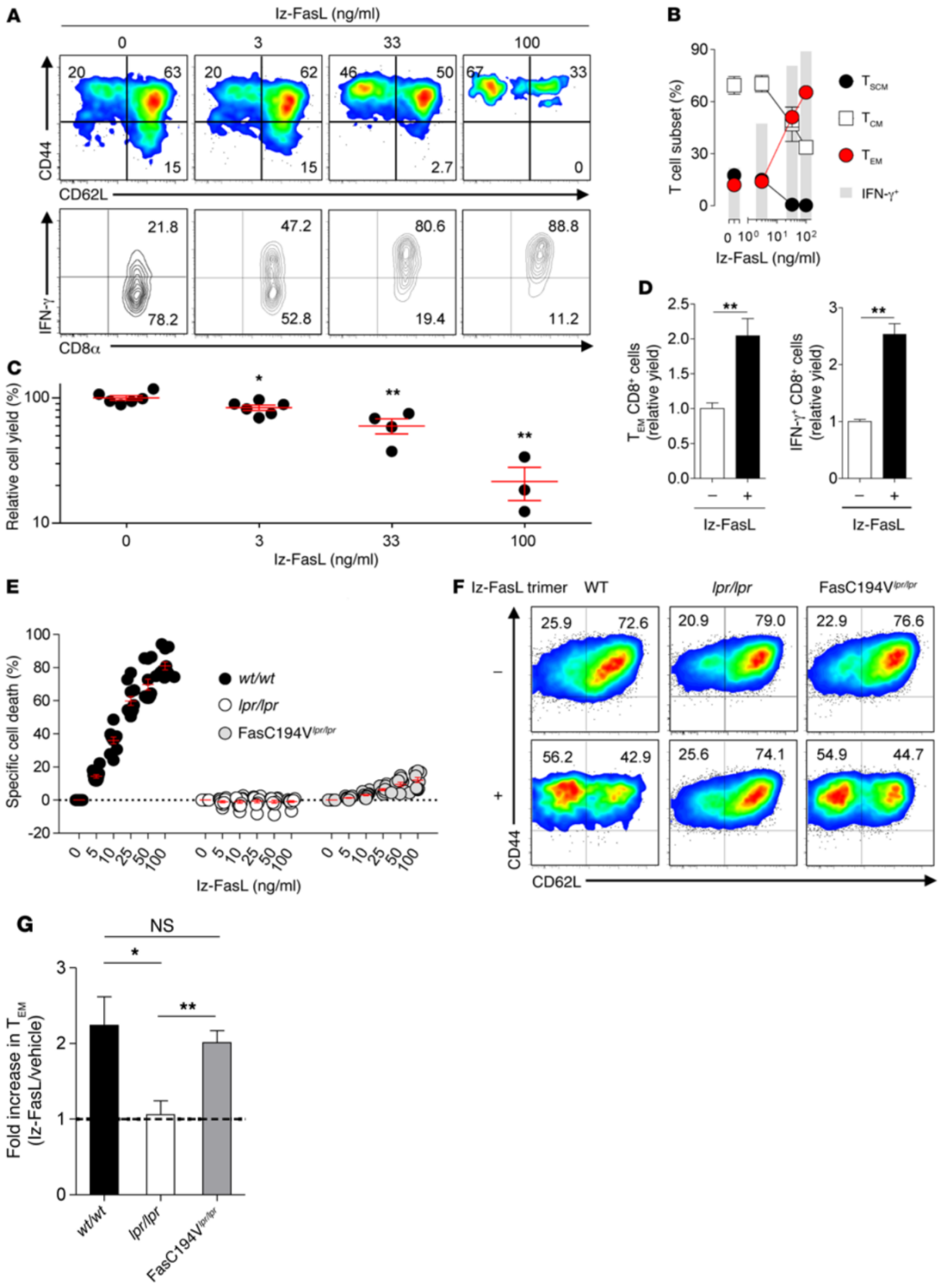

Figure 7 | Precocious differentiation is mediated by nonapoptotic Fas signaling. (**A**) Representative FACS plots and (**B**) bar graph summarizing the distribution of T cell subsets and IFN-γ production in isolated TN cells primed with CD3/CD28-specific antibodies, IL-2, and indicated doses of lz-FasL for 6 days prior to analysis. Data shown are based on $n = 3$

Figure 7… independently maintained cultures/conditions. (**C**) Relative overall cell yield and (**D**) relative cell yield of TEM or IFN-γ+ cells, normalized to no lz-FasL treatment, of TN-derived cells grown in the presence of titrated amounts of lz-FasL (**C**) or 33 ng/ml lz-FasL (**D**); data shown in **C** and **D** are based on $n = 3–6$ and $n = 3$ independently maintained cultures/condition, respectively. (**E**) Specific cell death of activated CD8+ T cells derived from WT (*WT*/*WT*), *Lpr* (*lpr*/*lpr*), and FasC194Vlpr/lprmice following exposure to titrated amounts of lz-FasL or a vehicle control; $n = 11$ per condition/cell type. (**F**) Representative FACS plots demonstrating the frequency of TN-derived cell subsets and (**G**) bar graph demonstrating fold increase in TEM phenotype cells after *WT*/*WT*, *lpr*/*lpr*, or FasC194Vlpr/lpr CD8+ T cells were expanded with CD3/CD28-specific antibodies and IL-2 alone or with 40 ng/ml of lz-FasL for 6 days; $n = 6–9$ independently maintained cultures/cell type. Statistical comparisons performed using an unpaired 2-tailed Student's *t* test corrected for multiple comparisons by a Bonferroni adjustment. $*P < 0.05$; $**P < 0.01$. Results are representative of 6 (**A**), 2 (**C**–**E**), and 4 (**F** and **G**) independently performed experiments and are displayed as mean ± SEM. Experiments performed and analyzed by Anthony Leonardi, Tori Yamamoto, and Christopher Klebanoff. Figure and legend used with permission from the Journal of Clinical Investigation (Klebanoff et al., 2016).

As seen in Figures A, B, and D treatment of WT cells with Fas-lz induces a functional differentiation phenotype, as measured by the markers CD44, CD62L, and by cytokine release. Indeed, treatment of WT cells with Fas-lz will induce their death, but the differentiation phenotype is preserved in C194V mutant T cells lacking Fas-mediated apoptosis (Figures 7 E, F, G). Taken together, these experiments show that lz-FasL trimer induces cell differentiation and death in WT murine CD8+ T cells, differentiation in C194V CD8+ T cells, and has no effect on lpr CD8+ T cells. Furthermore, the data suggests the change in the population of cells in culture to Effector Memory is not due to selective deletion of Naive T cells, but rather differentiation, due to the lack of death observed in the C194V T cells.

4.2 Fas Signaling Causes T Cell Differentiation in Human CD8+ T Cells

As the effect seen in murine T cells may be exclusive to them and not human T cells, in order to investigate the effect of Fas signaling in human T cells, CD8+ Naive T cells were separated from PBMCs via negative selection, stimulated with OKT3 and CD28, and cultured for 7 days with lz-FasL or vehicle (methods 7.2, 7.8, and 7.9). Cells were analyzed by flow cytometry to assess their differentiation (method 7.3) (Figure 8 A, B). Since there are not C194V mutants where the apoptosis and differentiation effect can be teased apart, specific cell death was analyzed according to differentiation subset after treatment with Fas-lz (Figure 8 C, D).

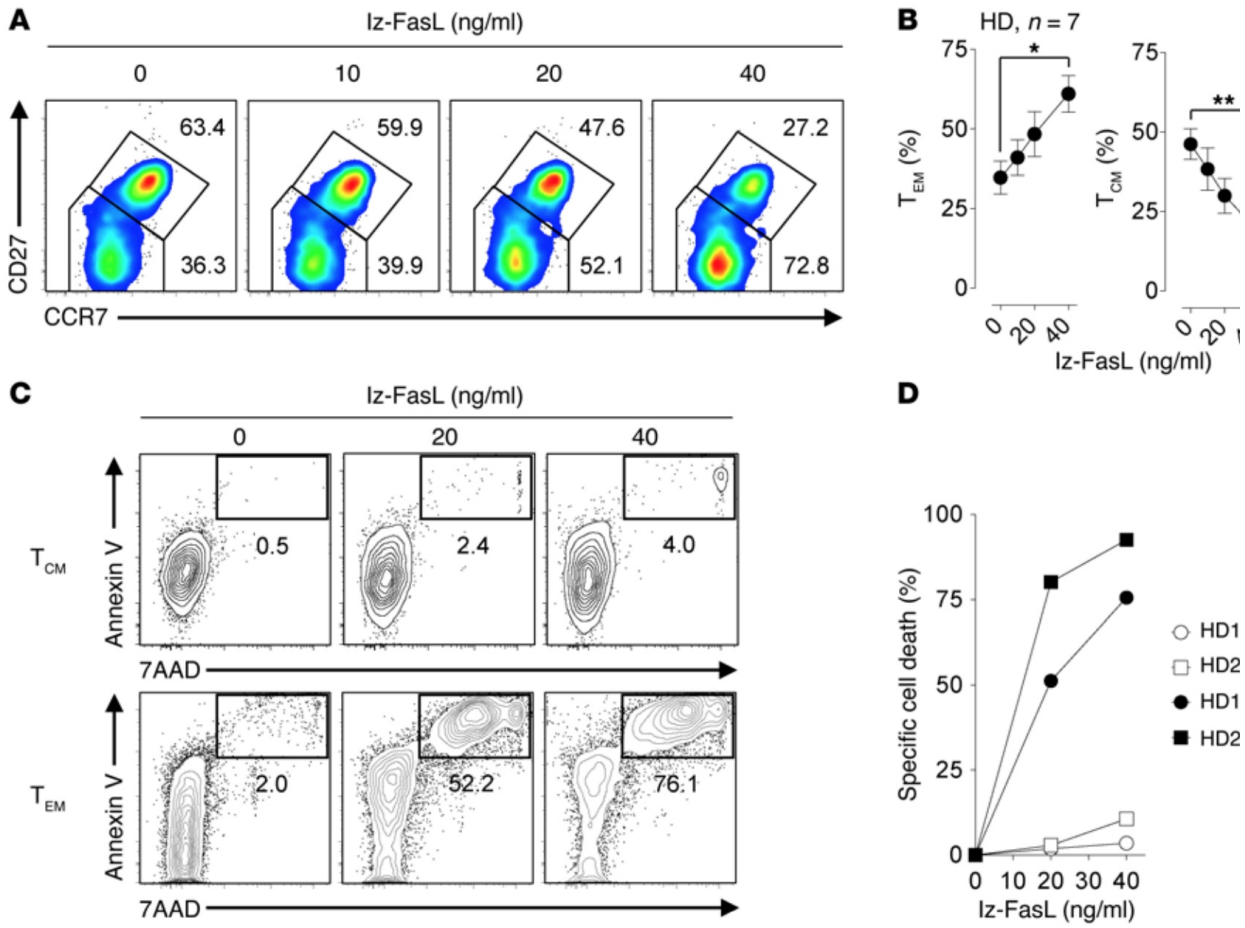

Figure 8 | Fas signaling promotes the differentiation of human CD8+ T cells. (**A**) Representative FACS plots and (**B**) summary graph showing the distribution of CD8+ T cell subsets 7 to 10 days after peripheral blood CD8+ T cells from HD were stimulated with CD3/CD28-specific antibodies, IL-2, and indicated concentrations of lz-FasL. Results shown after gating on viable CD8+lymphocytes from *n* = 7 HD. TCM = CD8+CD45RO+CCR7+CD27+, TEM = CD8+CD45RO+CCR7–CD27–. (**C**) Representative FACS plots and (**D**) summary graph displaying the induction of lz-FasL specific cell death after gating on TCM and TEM cells stimulated with indicated concentrations of lz-FasL for 12 hours. Cells that coordinately stained for 7-AAD and annexin V were considered apoptotic. Statistical comparisons performed using an unpaired 2-tailed Student's *t* test corrected for multiple comparisons by a Bonferroni adjustment. **P*< 0.05; ***P* < 0.01. Data shown are representative of 7 (**A** and **B**) and 2 (**C** and **D**) independently performed experiments with results displayed as mean ± SEM. Experiments performed and analyzed by Tori Yamamoto and Christopher Klebanoff. Figure and legend used with permission from the Journal of Clinical Investigation (Klebanoff et al., 2016).

Taken together, when given that lz-FasL promotes the downregulation of CD27 and CCR7 during cell culture in a titratable fashion (Figure 8 A, B), which is not dependent on a population-specific cell deletion via apoptotic induction (Figure 8 C, D), it can be concluded that Fas stimulation results in CD8+ T-cell differentiation in human cells.

4.3 Paracrine T-cell to T-cell Fas Signaling Causes T Cell Differentiation

In order to test a possible role of FasL acting in a paracrine manner, a 1:1 coculture of Memory T cells stimulated with Naive T cells was made with use of congenic markers to track these two populations of cells (method 7.9). In the following experiment, naive alone, and naive and memory CD8+ murine T cells were stimulated with CD3/CD28 and cultured for 7 days with anti-FasL blocking antibody or IGG (methods 7.2, 7.4, 7.8, and 7.9). After 6 days of coculture, phenotypes of the cells were analyzed by flow cytometry (method 7.3) (Figure 9A) and subset differences calculated between groups (Figure 9B). In order to measure effector function, cells were restimulated on Day 6 and measured for effector cytokine release (method 7.3) (Figure 9C). In order to test the possibility the paracrine differentiation effect was not FAS dependent, Naive Fas deficient T cells were concurrently cocultured with WT Memory T cells as described and analyzed by flow cytometry (methods 7.2, 7.3, 7.4, 7.8, 7.9, and 7.18) (Figure 9D).

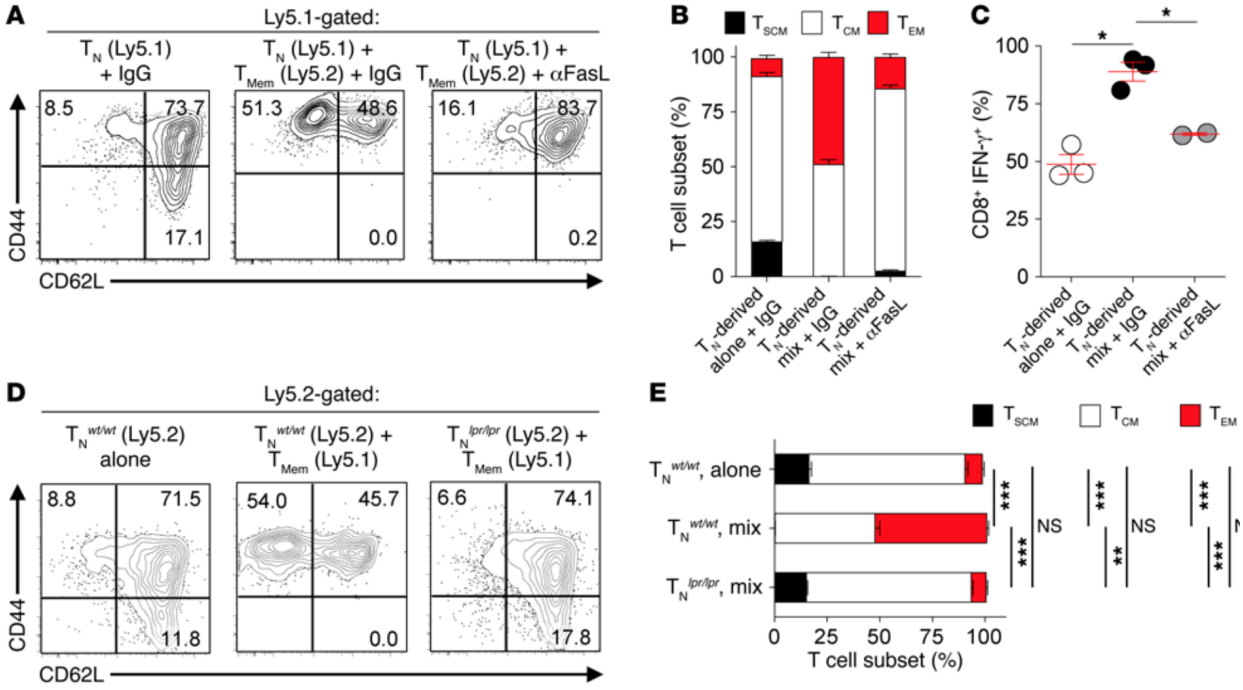

Figure 9 | Paracrine T-cell to T-cell Fas Signaling Causes T Cell Differentiation. (**A**) Representative FACS plots, (**B**) summary bar graph, and (**C**) scatter plot demonstrating T cell subset frequencies or percentage of IFN-γ+CD8+ T cells 6 days following priming of Ly5.1+ TN alone or in a 1:1 mixture with Ly5.2+ TMem with CD3/CD28-specific antibodies, IL-2, and a blocking antibody against FasL (αFasL) or isotype (IgG) control. (**D**) FACS analysis and (**E**) bar graph summarizing the distribution of CD8+ T cell subsets 6 days following priming of Ly5.2+

Figure 9…WT TN pmel-1 (TNWT/WT) or *lpr*/*lpr* TN pmel-1 (TN*lpr/lpr*) cells alone or in the presence of a 1:1 mixture with WT Ly5.1+ TMem. All results shown as mean ± SEM with $n = 2–3$ per indicated condition or cell type. Statistical comparisons performed using an unpaired 2-tailed Student's *t*test corrected for multiple comparisons by a Bonferroni adjustment. $*P < 0.05$; $**P < 0.01$; $***P < 0.001$. Data shown are representative of 14 (**A** and **B**), 4 (**C**), and 3 (**D** and **E**) independently performed experiments. Experiments performed and analyzed by Anthony Leonardi and Christopher Klebanoff. Figure and legend used with permission from the Journal of Clinical Investigation (Klebanoff et al., 2016).

This experiment reveals that T cells have the ability to cause differentiation in a paracrine manner, where lz-FasL expressed by memory T cells may act upon lesser differentiated counterparts and push them toward effector status, which can be abrogated with a lz-FasL blocking antibody (Figure 9 A, B, C). Given the absence of the effect when the naive T cell population does not express a functional Fas receptor as is the case in lpr/lpr mice, this phenomenon can be concluded to be a Fas- mediated effect, and not an effect of lz-FasL or lz-FasL on another receptor (Figure 9 D, E).

4.4 Fas-mediated Differentiation is Dependent Upon AKT

To determine whether the differentiation that is conferred by the paracrine FasL signalling is AKT dependent, naive WT murine CD8+ T cells were stimulated and cultured for 24 hours with and without the presence of memory T cells (methods 7.2, 7.4, 7.8, and 7.9). These cells were analyzed by flow cytometry for phosphorylation at residues T308 and S473 on AKT and S6 Kinase and their Mean Fluorescence Intensities compared to baseline (method 7.3) (Figure 10 A, B, C). To investigate a possible change in genes associated with lymphocyte maturation, expression levels were analyzed and compared during stimulation (Figure 10D). In order to analyze the effect of CD95 signaling without memory T cells, to be sure the effect on AKT in the naive cells was not mediated by cytokines or other agents the memory T cells, naive WT murine CD8+ T cells were stimulated with indicated amounts of lz-FasL with AKT inhibitor or vehicle (method 7.9). 24 hours after stimulation, cells treated with titrating amounts of lz-FasL were analyzed for AKT T308 phosphorylation by western blot (method 7.14) (Figure 10E). At day 6 following stimulation, cells were analyzed by flow cytometry for 2-NBDG uptake to measure glycolytic metabolism as indicated by sugar uptake (method 7.3) (Figure 10 F, G) which is associated with increased differentiation and effector function. To determine whether the differentiation signal from lz-FasL can be abrogated with an AKT inhibitor, cells treated

with lz-FasL and AKT inhibitor were analyzed by flow cytometry for differentiation marker expression (method 7.3) (Figure 10H) and effector cytokine release following restimulation, with comparison of the subsets (Figure 10I) and the cytokine release (method 7.18) (Figure 10J).

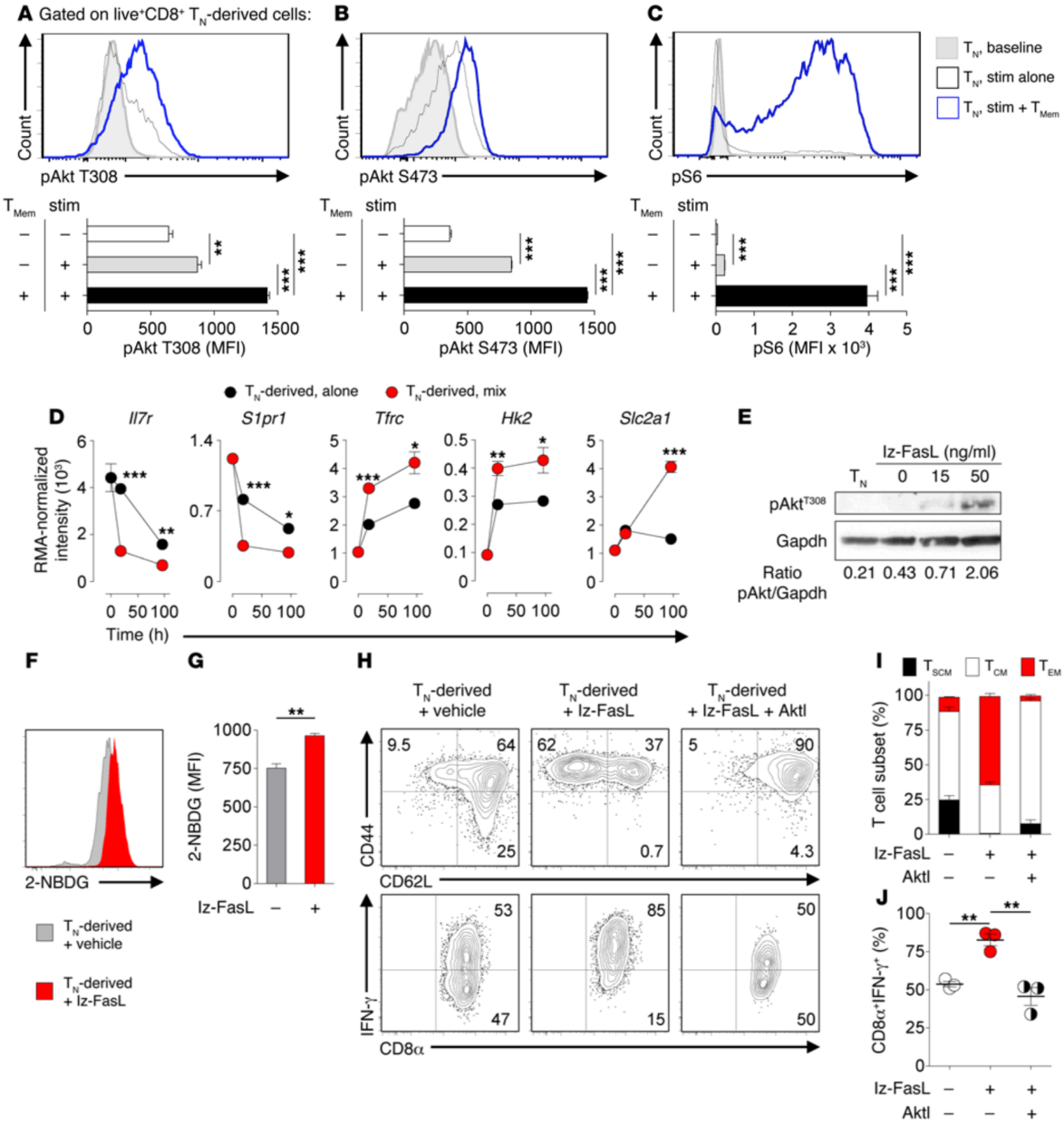

Figure 10 | Precocious differentiation is associated with augmented AKT signaling. Representative FACS histograms and summary bar graphs demonstrating the mean fluorescence intensity of (**A**) pAKT T308, (**B**) pAKT S473, and (**C**) pS6 in Ly5.2+CD8+ TN cells at rest or 24 hours after stimulation with CD3/CD28-specific antibodies alone or in a 1:1 mixture with Ly5.1+ TMem cells. Data shown after gating on live+Ly5.2+CD8+ cells. (**D**) RMA-normalized intensity Figure 10… showing expression of *Il7ra*, *S1pr1*, *Tfrc*, *Hk2*, and *Slc2a1* in resting TN cells, TN cells primed alone, and TN cells primed in a 1:1 mixture with TMem cells. (**E**) Western blot and densitometry analysis of pAKT T308 and GAPDH in resting TN or TN cells primed for 24 hours

Figure 10… with CD3/CD28-specific antibodies and titrated doses of lz-FasL. (**F**) Representative FACS plot and (**G**) summary scatter plot showing 2-NBDG expression in TN cells primed alone for 6 days with CD3/CD28-specific antibodies, IL-2, and lz-FasL (50 ng/ml) or vehicle control. Data shown after gating on live+CD8+ lymphocytes. (**H**) Representative FACS plots, (**I**) summary bar graph demonstrating the frequency of CD8+ T cell subsets, and (**J**) scatter plots showing IFN-γ production in TN cells primed with CD3/CD28-specific antibodies, IL-2, and lz-FasL (50 ng/ml) in the presence or absence of an inhibitor of AKT1/2 (AKTI) for 6 days. Statistical comparisons performed using an unpaired 2-tailed Student's *t* test corrected for multiple comparisons by a Bonferroni adjustment. $*P < 0.05$; $**P < 0.01$; $***P < 0.001$. All data shown are displayed as mean ± SEM. Experiments performed with $n = 3$ per condition/time point in **A**–**D** and **F**–**J**. All data shown are representative of 2 independently conducted experiments. Experiments performed and analyzed by Anthony Leonardi, Tori Yamamoto, Robert Eil, and Christopher Klebanoff. Figure and legend used with permission from the Journal of Clinical Investigation (Klebanoff et al., 2016).

These data reveal that the differentiation induced by memory cells on naive cells results in the phosphorylation (activity of AKT) at residues T308 and S473, and the activation of pS6 which is associated with increased metabolism, giving the possibility these cells will be more glycolytic (Figure 10 A, B, C). Additionally, these effects on differentiation are congruent with the mRNA levels of differentiation-related genes (Figure 10D). Furthermore, this effect on the phosphorylation state of AKT can be seen by western blot with use of lz-FasL in lieu of memory cells (Figure 10E) with an effect seen additionally on glucose uptake (Figure 10 F, G). The necessity of AKT signaling to propagate the differentiation induced by lz-FasL is also maintained (Figure 10 H, I, J). To summarize the data thus far, paracrine Fas- mediated differentiation is AKT dependent, and Fas-induced differentiation also increases the glycolytic activity of cells.

4.5 Fas Signaling Controls T Cell Differentiation and Attenuates Adoptive Immunotherapy Efficacy

In order to test the efficacy of T cell populations with and without Fas signaling in a tumor-treatment model of adoptive immunotherapy, murine Pmel-1 CD8+ T cells were stimulated as described (methods 7.2, 7.4, 7.8, and 7.9) in groups consisting of Naive CD8+ T cells alone, Naive CD8+ T cells with lz-FasL, Naive and memory CD8+ T cells in a 1:1 mixture with IGG antibody, and Naive and memory CD8+ T cells in a 1:1 mixture with anti-FasL blocking antibody. After culture expansion, B16 melanoma tumor-bearing mice were treated with a 6 Gy dose of radiation, intravenous rVV-gp100, and infused with 2.5×10^5 cells (method 7.7). IL-2 support was administered intraperitoneally once a day

for three days, and tumors were measured at least once every three days (method 7.7) (Figure 11A). Following the experiment, survival was plotted and measured between conditions (Figure 11B). Given that a change in efficacy could be due to the failure of adoptively transferred lz-FasL treated T cells to engraft in the host, 18 hours after infusion, a small amount of blood was taken from the tail vein of mice and the proportion of Pmel-1 CD8+ lymphocytes was measured by flow cytometry (method 7.1, 7.3) (Figure 11C). To illustrate the effect between CD62L expression and efficacy of adoptively transferred cells, a linear regression analysis was performed (method 7.18) (Figure 11D).

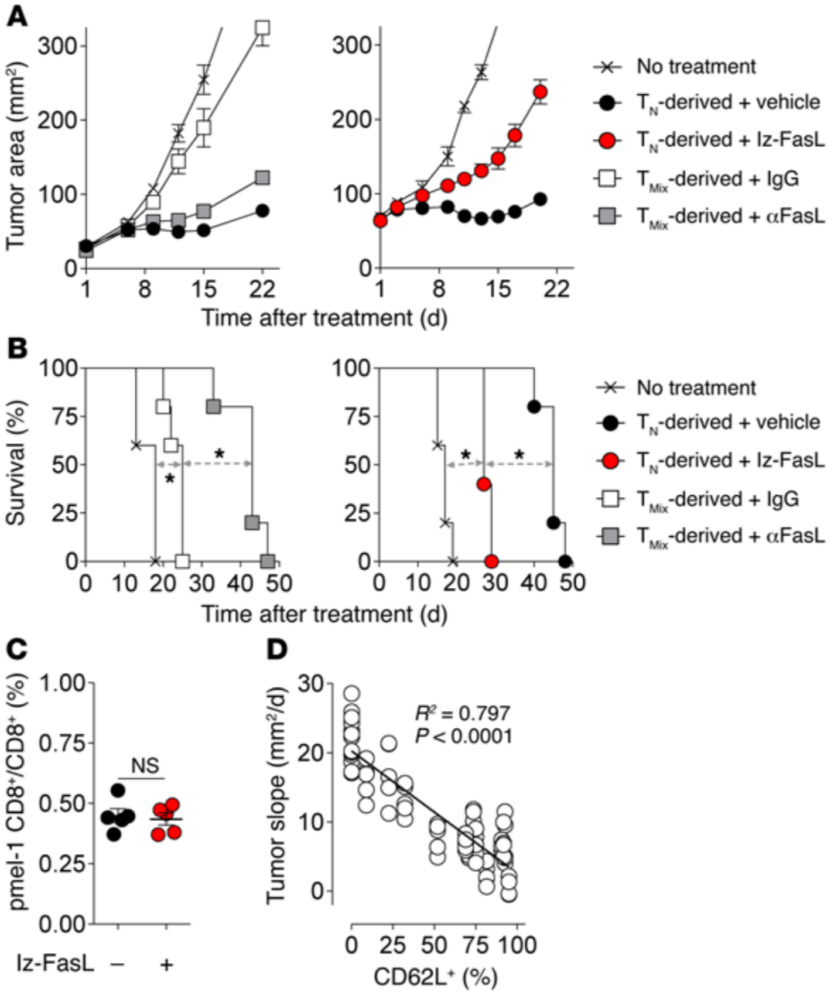

Figure 11 | Fas signaling controls T cell differentiation and influences adoptive immunotherapy efficacy. (A) Tumor regression and (B) animal survival of mice bearing 10-day established s.c. B16 melanomas treated with 2.5 × 105 TN-derived pmel-1 cells primed alone, with lz-FasL (50 ng/ml), or with TMem in the presence of αFasL or IgG control. Viable cells were isolated using a density separation media before infusion. All treated mice received 6 Gy irradiation prior to cell infusion in addition to i.v. rVV-gp100 and 3 days of i.p. IL-2. Tumor treatment experiments performed with n = 5 mice/group. TMix, TN cells primed with TMem cells in a 1:1 mixture. (C) Engraftment efficiency of Thy1.1+ TN-derived pmel-1 cells (3 × 105) primed alone or with lz-FasL 18 hours following i.v. adoptive transfer into nonirradiated Ly5.2+ hosts; n =

Figure 11… mice/group. (D) Correlation between the slope of tumor growth and CD62L expression at the time of cell transfer on TN-derived pmel-1 cells primed alone with either lz-FasL (50 ng/ml), vehicle control, or with TMem and either αFasL or IgG. Pooled results from 2 independently performed experiments displayed using n = 4–10 mice per condition. Statistical comparisons performed using an unpaired 2-tailed Student's t test or log-rank test for animal survival. *P < 0.05. Data shown are representative of 2 independent experiments with results displayed as mean ± SEM. Experiments performed and analyzed by Anthony Leonardi and Christopher Klebanoff. Figure and legend used with permission from the Journal of Clinical Investigation (Klebanoff et al., 2016).

Given the results of this data, abrogation of Fas signaling in heterogenous populations of T cells which contain naive and memory subsets is beneficial as measured by the efficacy of tumor immunotherapy (Figure 11 A, B). Furthermore, attenuation seen in the therapy by the addition of lz-FASL to naive cultures is not due to an engraftment failure (Figure 5C). Interestingly, the rate of tumor growth, or tumor slope, is correlated with the CD62L expression of the T cells used prior to infusion (Figure 11D). Taken altogether, Fas inhibition represents a novel efficacious method of enhancing the efficacy of tumor immunotherapy, as demonstrated in a murine model.

4.6 AKT Inhibition prevents differentiation of T cells

To test the phenotype conferred to T cells stimulated and cultured while under AKT inhibition, human T cells were isolated from blood, stimulated with anti-CD3 (OKT3) in IL-2 containing media with and without AKT inhibitor, and transduced with the CD19 CAR on Day 2, and cultured until day 10 (method 7.10) (Figure 12A) (Klebanoff et al., 2017). In order to understand the pathways affected by inhibition, groups were stained for phosphorylation state of specific signaling proteins at three timepoints: before stimulation, and 5 and 10 minutes following stimulation at points in the AKT/mTOR pathways (Figure 1B) and MAPK pathway (method 7.12) (Figure 12C). Following a culture period of 10 days, the cell expansion was calculated and compared between groups (method 7.18) (Figure 12D), and transduction efficiency (Figure 12E) and CD62L expression (Figure 12F, G) was analyzed by flow cytometry (method 7.12).

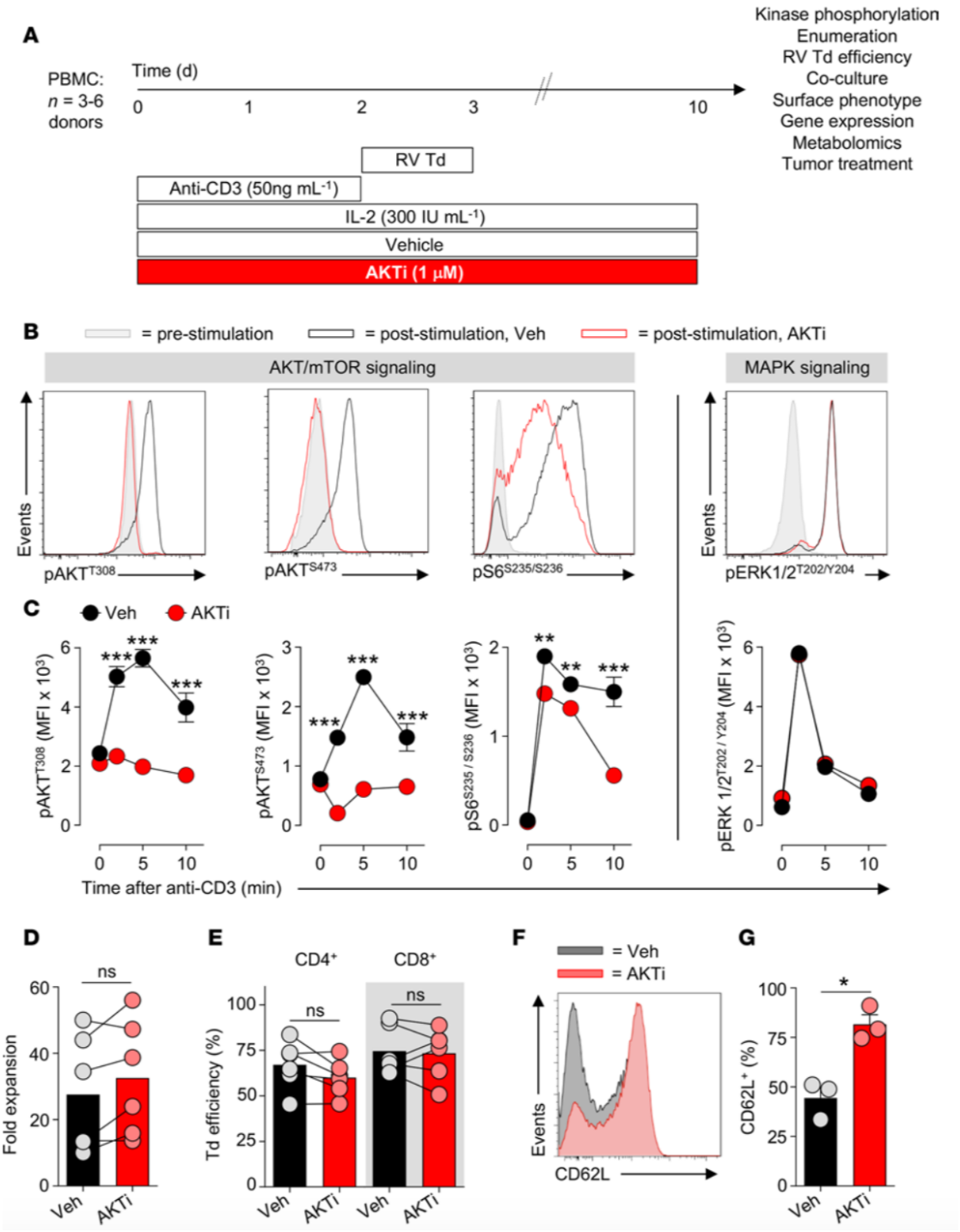

Figure 12 |Pharmacologic inhibition of AKT signaling permits expansion of CD62L-expressing receptor-engineered human peripheral blood T cells. (**A**) Schema for the anti-CD3 (50 ng ml–1) activation, retroviral transduction (RV Td), and expansion of human peripheral blood T lymphocytes (PBL) in the continuous presence of IL-2 (300 IU ml–1) and AKT inhibitor VIII (AKTi; 1 μM) or vehicle control (Veh). (**B**) Representative phosphoflow cytometry plots and (**C**) graphical summary of the time-dependent phosphorylation of kinases involved AKT/mTOR or MAPK signaling in PBL expanded in the presence or absence of AKTi immediately prior to and following stimulation with an anti-CD3 antibody. Results from 1 of 2 representative experiments are displayed. (**D**) Fold expansion and (**E**) transduction efficiency of unfractionated PBL genetically engineered with a second-generation 28z anti-CD19 chimeric antigen receptor (CAR) following ex vivo expansion over 10d in the continuous presence IL-2 and AKTi or Veh. Pooled

Figure 12… results from 6 independent donors are shown after gating on viable, transduced CD3+CD4+ and CD3+CD8+ cells. (**F**) Representative FACS plot and (**G**) graphical summary of CD62L expression on CAR-modified PBL expanded for 10d in AKTi or Veh control. Results shown in panels **D**–**G** are based on patient-derived samples, while results in panels **B** and **C** used healthy donor (HD) T cells. Data in panels **C**–**E** and **G** are presented as mean ± SEM with $n = 3$, $n = 6$, $n = 6$, and $n = 3$ per condition, respectively. All statistical comparisons were performed using an unpaired 2-tailed Student's t test. ***$P < 0.001$; **$P < 0.01$; *$P < 0.05$. Experiments performed and analyzed by Joseph Crompton, Robert Eil, and Christopher Klebanoff. Figure and legend used with permission from JCI Insight (Klebanoff et al., 2017).

Interestingly, the data revealed as expected the AKT and mTOR pathways were affected as measured by phosphorylation status by the AKT inhibitor, but the MAPK/ERK pathway was unaffected by the addition of AKT. (Figure 12 B,C). As the MAPK pathway is required for cell survival and proliferation, this would allow for cells to continue expanding and multiplying at normal rates, as seen in Figure 12 D. As the retrovirus used for transduction requires cells to be proliferating for optimal rates, likely due to the unhindered proliferation between groups there was also no difference in the CD19 CAR transduction between them (Figure 12E), however the phenotype difference of CD62L expression, which denotes greater memory and less differentiation was indeed significantly discrepant (Figure 12 F, G). Taken together, this evidence strongly suggests AKT inhibition enables cell proliferation while holding back cell differentiation by holding back the AKT/mTOR pathways and leaving MAPK unperturbed.

4.7 AKT Inhibition Lowers Glycolytic Activity of CAR-T Cells

Given the observation that the metabolic state of CAR-T cells correlates with tumor-treatment response (Kawalekar et al., 2016), the metabolic state of AKT treated cells was further characterized in order to determine fitness. T cells from healthy human donors were isolated, stimulated, and transduced with the CD19 CAR as described (method 7.10). Following 5 days of stimulation and culture, cells were harvested and assayed via metabolomic analysis to observe the levels of intracellular metabolites (method 7.15) (Figure 13 A, B) and analyzed by flow cytometry for 2-NBDG uptake after co-incubation (method 7.15) (Figure 13C). Cells treated with AKT inhibitor or vehicle were plotted by their principal components in principal component analysis (PCA) revealed by metabolomic analysis (method 7.15) (Figure 13A), and lactate production (Figure 13B). To test if the genes associated with glycolysis were changed in expression and function by AKT inhibition, CD19 CAR-T cells were cultured for 10 days and analyzed by seahorse

for their extracellular acidification rate (ECAR) (method 7.15) (Figure 13D) and also analyzed by mRNA for expression of key metabolic genes involved in glycolysis and lactate transport (method 7.14) (Figure 13E).

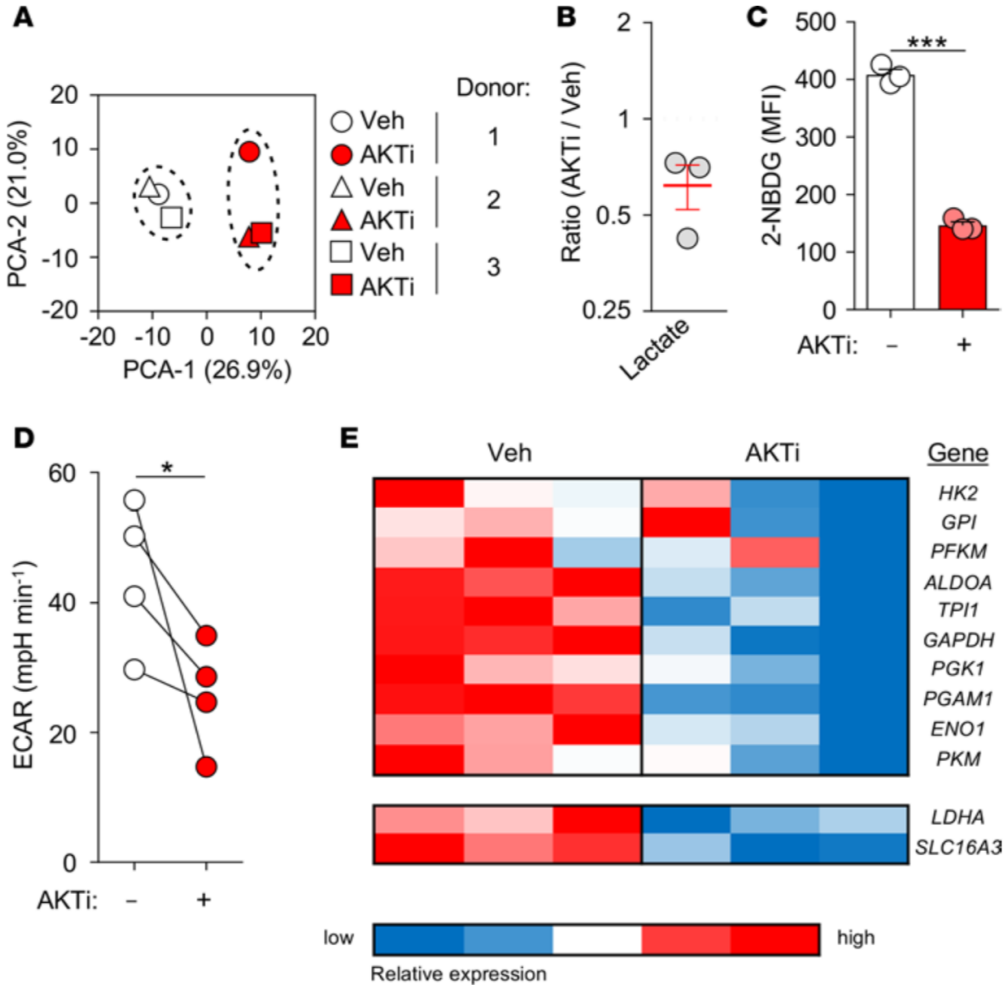

Figure 13 | AKTi limits the acquisition of a glycolytic metabolism in human peripheral blood T cells transduced with an anti-CD19 CAR. (A) Two-dimensional principal component analysis (PCA) visualizing the variation in 308 metabolites detected using a metabolomic assay in anti-CD19 chimeric antigen receptor (CAR) transduced T cells expanded in AKTi or vehicle control (Veh). Percentages indicate the amount of variance captured within each principal component. Results are shown from 3 independently evaluated donors using the average of $n = 5$ replicates per condition and donor. (B) Ratio of lactate, an end glycolytic intermediate, detected in anti-CD19 CAR transduced T cells expanded in the continuous presence of AKTi versus Veh. The mean ratio ± SEM from $n = 3$ independently evaluated donors is shown with the dashed line indicating a lactate ratio of 1. (C) 2-(N-[7-nitrobenz-2-oxa-1,3-diazol-4-yl]amino)-2-deoxyglucose (2-NBDG) uptake and (D) extracellular acidification rate (ECAR) 5d after stimulation and expansion of peripheral blood T cells in the continuous presence of AKTi or Veh control. Results shown in panel C are representative of 3 independently performed experiments; results in panel D are based on cultures from $n = 4$ independently evaluated donors. (E) Heat map of gene expression for the 10 enzymes involved in glycolysis and the 2 primary lactate exporters, *LDHA* and *SLC16A3*, found in lymphocytes. Each column represents the average expression of a gene from 3 independently evaluated patient donors, and each row represents the indicated gene. Red and blue colors indicate

Figure 13… relative increased and decreased expression, respectively. Data shown in panels A, B, and E are from patient-derived T cells, and panels C and D are from healthy donors (HDs). Statistical comparisons in panels C and D were performed using an unpaired 2-tailed Student's *t* test. ***$P < 0.001$; *$P < 0.05$. Experiments performed and analyzed by Anthony Leonardi, Madhu Sukumar, Joseph Crompton, and Christopher Klebanoff. Metabolomics performed by Metabolon Corporation. Figure and legend used with permission from JCI Insight (Klebanoff et al., 2017).

As revealed by the data, CAR-T cells treated with the AKT inhibitor have a consistent metabolic signature and cluster in PCA (Figure 13A). These cells also produce less lactate (Figure 13B) and consume less glucose (Figure 13C) compared to vehicle treated cells. As seahorse ECAR analysis measures hydrogen proton concentration in the media as it is released from T cells, it is used as an indirect measurement of lactate and glycolytic flux, which the data revealed AKT treated CD19 CAR-T cells to be significantly less reliant on acidic metabolic pathways (Figure 13D). Indeed, AKT treated cells had significantly less expression of glycolytic enzymes (Figure 13E). Taken on the whole, these data reveal that AKT treatment increases the metabolic fitness of T cells used for CD19 CAR-T therapy, which correlates with tumor response (Kawalekar et al., 2016).

4.8 AKT Inhibition Withholds T Cell Differentiation and Promotes FOXO1 Nuclear Localization

Given the pronounced changes in differentiation phenotypes associated with AKT inhibition, a more comprehensive approach to categorizing the genetic program changes was taken. Human CD19 CAR-T cells were manufactured as described previously through isolation from peripheral blood, stimulation with OKT3 and anti-CD28, and retroviral transduction in the presence of AKT inhibitor or vehicle (method 7.10). Transcriptomic analysis was performed on day 10, which yielded a consistent pattern of gene clustering for AKT treated, untreated, and baseline control groups (method 7.16) (Figure 14A). Differential expression of top genes from transcriptomic analysis were listed, many directly correlating with T cell differentiation and phenotypic markers, including *SELL*, which encodes CD62L (Figure 14B). These differentially expressed genes were grouped under categories of interest including genes which are controlled by a single transcription factor (FOXO1), genes encoding costimulatory proteins, genes encoding effector molecules, and genes involved in apoptosis (Figure 14B). mRNA analysis of expression levels of genes specifically associated with effector function and differentiation was performed (method 7.16) (Figure 14C). As AKT inhibition created a discrepant expression

profile of many genes responsible for differentiation phenotype which are under control of the transcription factor FOXO1, and since AKT has been shown in cancer cell lines to inactivate FOXO1 via phosphorylation which traps FOXO1 in the cytosol and prevents migration to the nucleus, confocal microscopy was performed in order to localize the FOXO1 in AKT treated and untreated cells to the nucleus by permeabilizing the membrane of the cells and incubating with FOXO1 specific antibody (labeled with hoescht) or cytoplasm (labeled with phalloidin), the labeled with a secondary fluorescent antibody targeting the FOXO1 primary (method 7.17) (Figure 14D). The ratios of nuclear vs. cytoplasmic concentrations of FOXO1 were calculated (Figure 14E), and the expression level of FOXO1 between groups was also measured in order to determine if it was a factor in any cytosolic vs. nuclear differences observed (methods 7.17, 7.18) (Figure 14F).

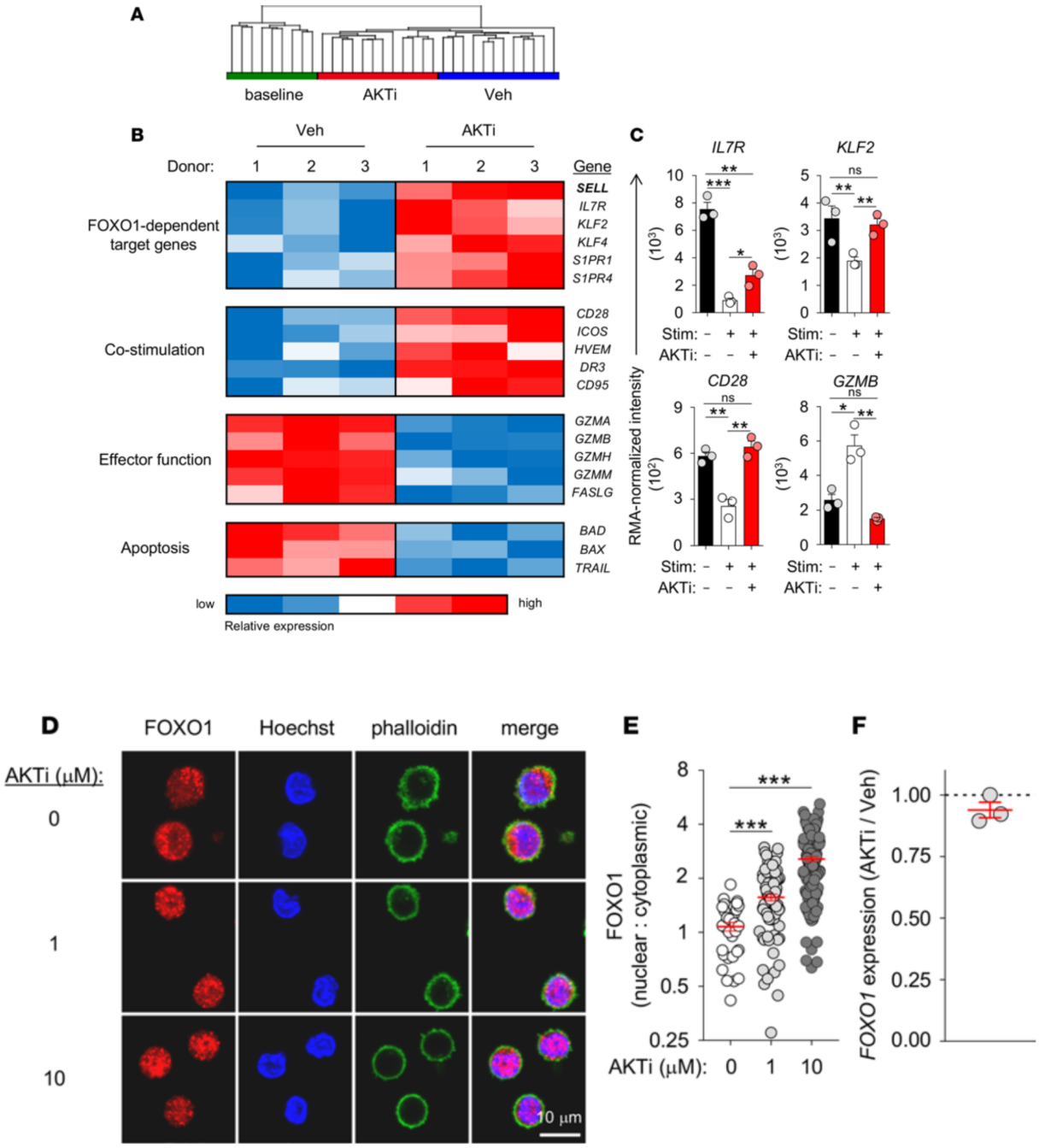

Figure 14 | Blockade of AKT signaling minimizes gene expression changes associated with human T cell differentiation and promotes nuclear accumulation of the transcription factor FOXO1. (**A**) Unsupervised hierarchical clustering of gene expression from peripheral blood T cells at baseline and 10d after stimulation, retroviral transduction (RV Td) with an anti-CD19 chimeric antigen receptor (CAR), and expansion in the continuous presence of IL-2 (300 IU ml–1) and AKT inhibitor VIII (AKTi; 1 μM) or a vehicle control (Veh). Clustering was based on all significantly expressed genes (1-way ANOVA, FDR-corrected $P < 0.05$) using a Pearson correlation. T cells were derived from 3 independent donors using an $n = 3–4$ replicates per donor, per time point, and per condition. (**B**) Heat map of expression for selected genes that are direct targets of the transcription factor FOXO1 or genes involved in T cell costimulation, effector function, and apoptosis. Red and blue colors indicate relative increased and decreased expression, respectively. Each column represents the average expression of a gene from an individual donor, and each row represents the indicated gene. (**C**) Robust multichip analysis–normalized (RMA-normalized) intensity of selected FOXO1-target genes and genes associated with T cell differentiation at

Figure 14… baseline and 10d after ex vivo expansion in the continuous presence of AKTi or Veh. The bar graphs represent the mean ± SEM of $n = 3$ overlaid biological replicates per condition from a single donor and are representative of experiments observed with all 3 independently analyzed donors. (**D**) Representative confocal immunofluorescence images and (**E**) summary graph quantifying the dose-dependent intranuclear accumulation of FOXO1 4d following T cell activation and expansion in indicated concentrations of AKTi or Veh control. Red, FOXO1; blue, Hoechst; and green, phalloidin. Scale bar: 10 μm. Data shown are representative of 2 independently performed experiments using 2 separate donors. (**F**) The ratio of gene expression levels for *FOXO1* in AKTi- versus Veh-treated cells from n=3 independently evaluated donors. Dashed horizontal line indicates an expression ratio of 1. Data shown in panels **A**–**C** and **F** are from patient-derived T cells, and panels **D** and **E** are from healthy donors (HDs). Statistical comparisons in panels **C** and **E** were performed using an unpaired 2-tailed Student's t test corrected for multiple comparisons by a Bonferroni adjustment. ***$P < 0.001$; **$P < 0.01$; *$P < 0.0167$. Experiments performed and analyzed by Anthony Leonardi, Joseph Crompton, and Christopher Klebanoff. Figure and legend used with permission from JCI Insight (Klebanoff et al., 2017).

Taken together, there is a consistent genetic program exhibited by treating CD19 CAR-T cells with an AKT inhibitor during stimulation and expansion with a differentiation profile that is pertinent to FOXO1. Furthermore, AKT's effect of cytoplasmic sequestration on FOXO1 can be abrogated by inhibiting AKT activity, as demonstrated by confocal microscopy. Based on this conclusion, it would be worth investigating whether the enforced activity of FOXO1 can overcome AKT's inhibitory effect on nuclear localization, and create a memory phenotype.

4.9 FOXO1 Expression Confers a Lesser-Differentiated T-cell Phenotype

Given that AKT can affect FOXO1 activity via phosphorylation at the T24, S256, and S319 residues, a mutant FOXO1 gene ($FOXO1^{AAA}$) was engineered by substituting Alanine at these residues which cannot be phosphorylated, and encoded into a retrovirus in order to enforce expression of $FOXO1^{AAA}$ (Figure 15 A, B). $FOXO1^{AAA}$ should remain unaffected by AKT due to the lack of AKT-dependent phosphorylation sites. Since FOXO1 is in control of the differentiation markers in an AKT-dependent manner, a discrepancy should be seen among AKT-dependent markers of differentiation between cells transduced with $FOXO1^{AAA}$ and control (empty) vector. To begin the experiment, PBMC from an individual human donor was isolated, stimulated with and without AKT inhibitor for each type of transduction, and transduced with the Retrovirus for $FOXO1^{AAA}$ alongside a group transduced with an empty vector with the congenic marker thy1.1 (method 7.10). Cells were analyzed by flow cytometry 5 days after stimulation for genes

associated with effector function and differentiation, and gated on the cells which were positive for the congenic marker thy1.1, denoting successful transduction (method 7.12) (Figure 15C). The percentage of specific subsets for each condition were determined through flow cytometry and compared (method 7.19) (Figure 15D).

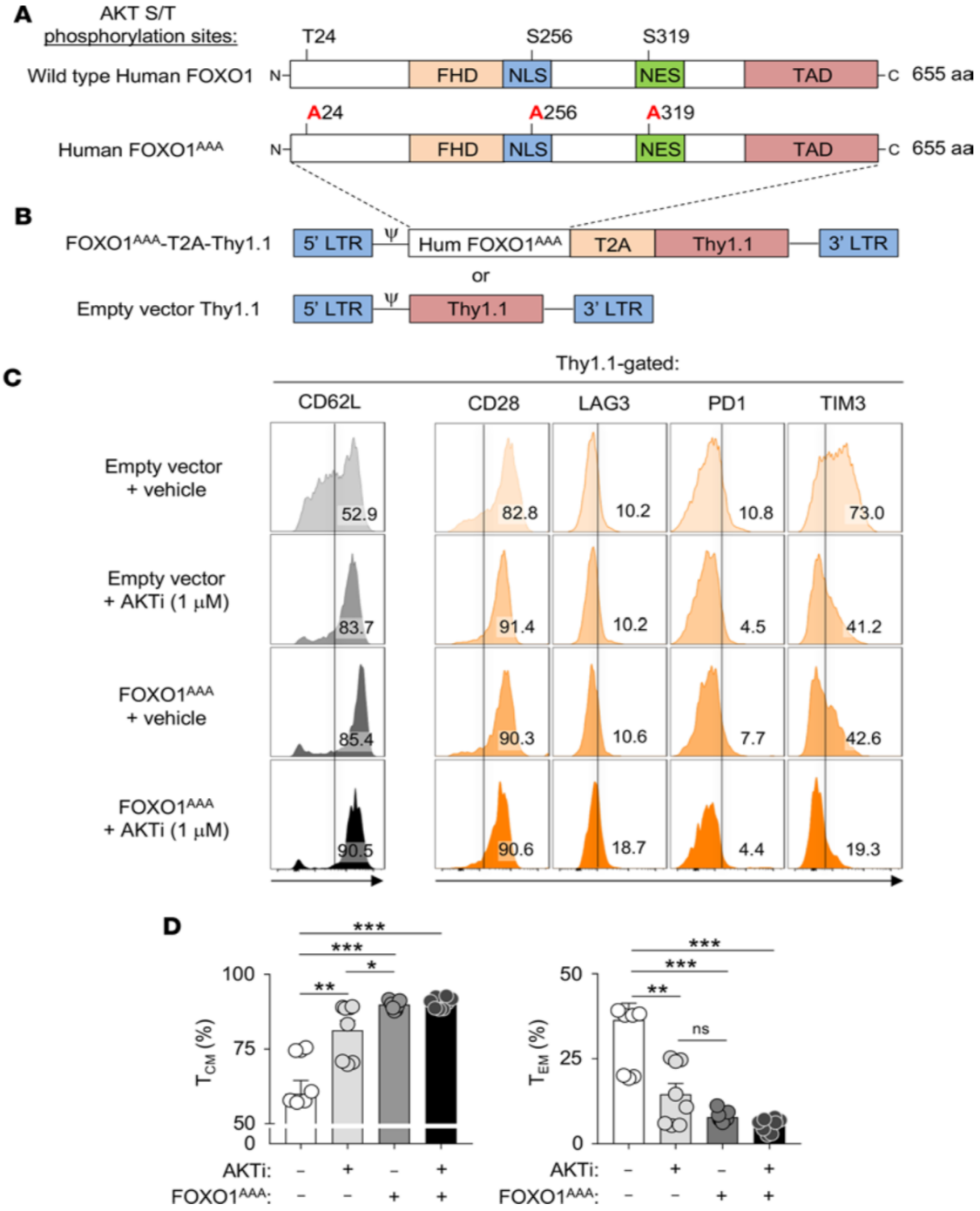

Figure 15 | Expression of a constitutively active form of FOXO1 augments CD62L expression independently of AKTi. (A) Schematic diagram of WT human FOXO1 protein highlighting 3 serine/threonine residues that serve as AKT phosphorylation sites and an alanine substituted variant (FOXO1AAA) refractory to AKT phosphorylation. Shaded boxes represent specific functional domains within the FOXO1 protein. FHD, forkhead domain; NLS, nuclear localization signal; NES, nuclear export signal; TAD, transcriptional activation domain. (B) Schematic illustration of the MSGV retroviral constructs containing FOXO1AAA and a Thy1.1 reporter separated by a T2A ribosomal skip sequence (FOXO1AAA-T2A-Thy1.1) or an empty vector Thy1.1 (Empty-Thy1.1) control. (C) Expression of CD62L, CD28, LAG3, PD1, and TIM3 on Thy1.1-gated T cells 5d after stimulation and retroviral transduction with FOXO1AAA-T2A-Thy1.1 or Empty-Thy1.1 control in the presence or absence of AKTi (1 μM) and IL-2 (300 IU ml–1). Results from 1 of 2 representative experiments are shown. (D) Summary bar graphs and overlaid individual data points

Figure 15… showing the distribution of TCM and TEM subsets in T cells expanded in the presence or absence of AKTi following transduction with FOXO1AAA-T2A-Thy1.1 or Empty-Thy1.1. Each bar graph represents the mean ± SEM of independent replicates from $n = 8$ independently performed experiments using healthy donor (HD) T cells. Statistical comparisons performed using an unpaired 2-tailed Student's t test corrected for multiple comparisons by a Bonferroni adjustment. $***P < 0.001$; $**P < 0.01$; $*P < 0.0167$. Experiments performed and analyzed by Anthony Leonardi, Smita Chandran, and Christopher Klebanoff. Figure and legend used with permission from JCI Insight (Klebanoff et al., 2017).

According to the data from this experiment, there is a FOXO1-dependent increase of CD62L expression even without the addition of AKT inhibitor, in the group of T cells transduced with $FOXO1^{AAA}$ even when compared to AKT inhibition alone (Figure 15D). Furthermore, $FOXO1^{AAA}$ transduction combined with AKT inhibition did not have an increased effect on retaining the memory phenotype when compared to AKT inhibition alone. Given the dominant effect of $FOXO1^{AAA}$, this data supports the conclusion that the abrogation of AKT mediated differentiation by use of the AKT inhibitor is FOXO1 dependent.

4.10 AKT Inhibition Augments CAR-T Cell Adoptive Immunotherapy

Given the benefits to metabolism and differentiation seen with the treatment of AKT inhibitor, testing the human CD19 CAR-T cells treated by AKT inhibitor in a xenograft model was performed to directly compare the *in vivo* tumor-killing efficacy of the cells. As described previously, human lymphocytes were isolated, stimulated, transduced with the CD19 CAR, and grown in the presence of AKT inhibitor or vehicle (method 7.10). These cells were then transferred at a rate of 1×10^6 into immunodeficient NOD scid γ (NSG) mice bearing acute lymphoblastic leukemia (ALL) as described (method 7.5, 7.6). Tumors were visualized using a luciferase reporter gene they expressed which was visualized by *in vivo* bioluminescent imaging (method 7.5) (Figure 16A). 35 days after treatment, survival was compared between groups (method 7.18) (Figure 16B).

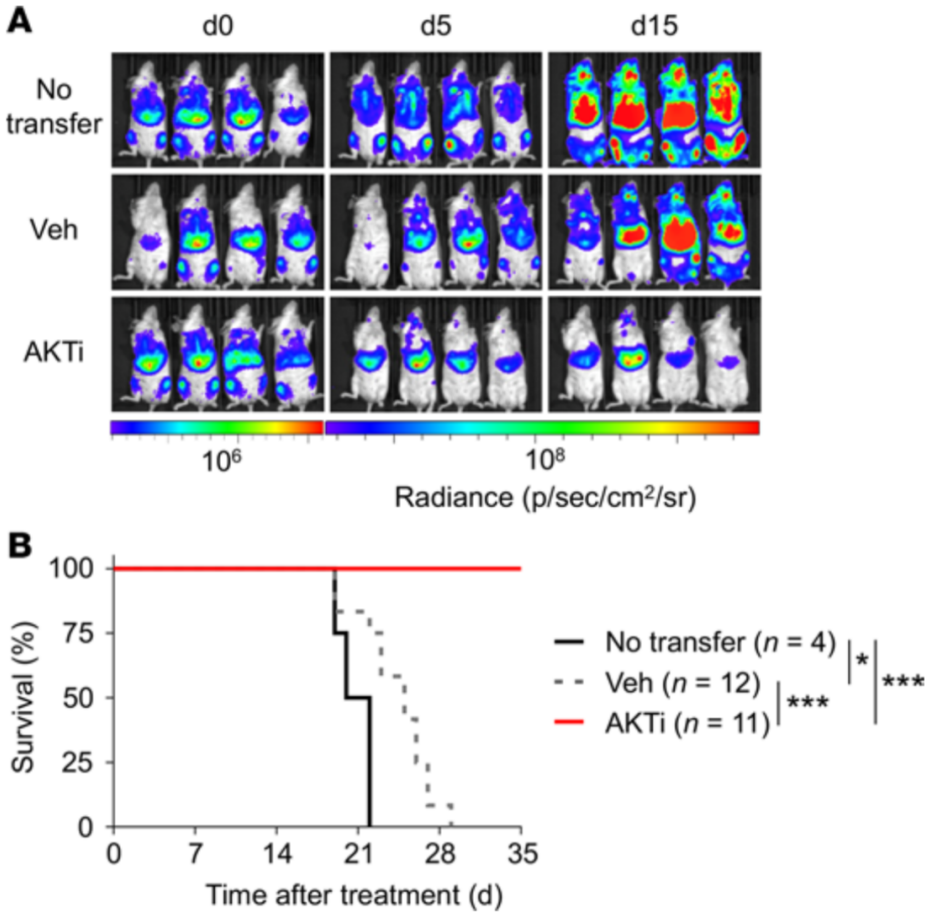

Figure 16 | Anti-CD19 CAR–modified T cells expanded in the presence of AKTi treat established leukemia superiorly to conventionally grown T cells. (A) In vivo bioluminescent imaging and (B) overall survival of NOD scid γ (NSG) immunodeficient mice bearing established, systemic, NALM6-GL leukemia xenografts following adoptive transfer of anti-CD19 chimeric antigen receptor–modified (anti-CD19 CAR–modified) peripheral blood T cells expanded in the presence of AKTi (1 μM) or vehicle (Veh) control. Data shown in panel A is from T cells using a patient donor that is representative of findings in all 3 patient donors; data shown in panel B are the pooled survival results from $n = 4–5$ mice per condition per donor using cells derived from 3 patient donors. Differences in overall survival were determined using the Mantel-Cox test. ***$P < 0.001$; *$P < 0.05$. Experiment performed and analyzed by Luca Gattinoni, Yun Ji, and Christopher Klebanoff. Figure and legend used with permission from JCI Insight (Klebanoff et al., 2017).

Given the significantly increased survival benefit of mice bearing ALL in a CD19 CAR-T xenograft model, it can be concluded that AKT inhibition yields CAR-T cells which are superior in tumor treatment efficacy, justifying the superior measurements of fitness by phenotypic markers of differentiation and metabolism.

5 COHESIVENESS OF THE PUBLICATIONS

The excerpted figures from the author's publications presented here represent a linear mechanism in T cell differentiation and its use to better the adoptive immunotherapy of cancer. As the datasets and narratives surrounding the findings that 1) T-cells differentiate via AKT (Leonardi and Crompton, 2012, Crompton et al., 2015, Klebanoff et al., 2017) and 2) T-cells differentiate via Fas (Leonardi AJ, 2012, Klebanoff et al., 2016) are vast, they expand several publications and represent four years of full-time investigation and employment at the NIH. Taking these findings and publications which span 5 years, three posters, and three separate papers into account, a stepwise pathway of T cell differentiation can be traced from T cell activation, to CD95 costimulation, to AKT phosphorylation, to the direct inhibition of the transcription factor FOXO1 which directly causes a memory/naive phenotype via expression of CD62L (Leonardi and Crompton, 2012, Leonardi AJ 2012, Yamamoto et al., 2015, Crompton et al., 2015, Klebanoff et al., 2016, Klebanoff et al., 2017). The figures presented in this thesis aim to highlight the linearity and logical progression of the discoveries. The discovery that AKT inhibition bettered T cells for adoptive immunotherapy, and the discovery that Fas signaling caused T cells to differentiate were both presented internally within the NIH by the author in 2012, and not published externally until 2015, 2016, and 2017. As there was an opportunity in commercialization of the invention of Fas blockade in T cells for adoptive immunotherapy, an invention report was issued by the National Institutes of Health detailing the application of the finding in 2012.

The points of intervention for withholding T cell differentiation presented in this work act in concordance. To be specific, the publication in January 2016 in JCI reveals that the signal caused by CD95 stimulation is propagated through AKT (Klebanoff et al., 2016, Figure 7). These mechanistic studies allow for the categorization of the Fas differentiation signal as a kind of co-stimulation upstream of the AKT signaling event, where the AKT-mediated differentiation signal can be attenuated with an AKT inhibitor, or prevented with antibody blockade of CD95L (Klebanoff et al., 2016). The data published in 2017 in JCI insight is a further development and application of the AKT project as pertaining to CAR-T cells (Klebanoff et al., 2017). In it, the pathway following AKT signaling is explored and the direct influence of AKT on transcription factors and their role in cell differentiation

uncovered, specifically by use of FOXO1 transduction, which is a transcription factor directly inhibited by AKT (Klebanoff et al., 2017, Figure 3).

Other publications by the author outside of the FAS and AKT project have similar goals in targeting tumor necrosis factor (TNF) family members in immunotherapies. For example, since TNF family members may be associated with toxicity following adoptive cell transfer, they may be antagonized during adoptive immunotherapy, as proposed in a recently published patent application (Leonardi AJ, 2018).

Other publications seek to optimize T cell function after adoptive transfer. The use of IL-12 in adoptive immunotherapy was such an effort, although it did not focus on the differentiation of T cells but rather their function in the tumor microenvironment (Kerkar et al., 2011). The use of ATRA as a conditioning regimen for T cell infusion related to T cell function and dendritic cell fate in tumor immunotherapy (Klebanoff et al., 2013).

In summary, all publications listed in this thesis pertain to fine-tuning T cell function for the immunotherapy of cancer.

6 CONTRIBUTION TO THE FIELD

This section will detail the two major contributions to the field made by the author, which have been reflected by the data and figures shown in the thesis. These contributions include the use of AKT inhibition in Adoptive T cell therapy and the paracrine differentiation of T cells by CD95 signaling. Altogether, the author has been cited 474 times for the sum of work in tumor immunotherapy (Fig. 15).

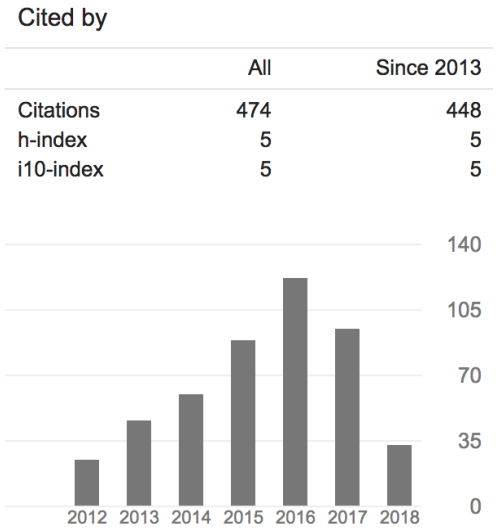

Figure 17 | Number of Citations of the Author's work

6.1 Use of AKT Inhibition in Adoptive T-Cell Therapy

The uncoupling of differentiation from proliferation and culture expansion is an invaluable ability in adoptive T cell immunotherapy (Crompton et al., 2014). Therapeutic outcomes are greatly affected by the level of differentiation and proliferative capacity of the T cells used (Rosenberg et al., 2011, Klebanoff and Gattinoni, 2012). The addition of a single small molecule to cell culture represents an unrivaled level of ease of implementation. As such, academic and commercial entities have quickly adopted the addition of an AKT inhibitor to T cell cultures for adoptive immunotherapy, with the first publication an internal poster session in the NIH for postbaccalaureate research fellows in 2012 (Leonardi and Crompton, 2012). As of April 2018, the first external publication in 2015 detailing use of AKT inhibition for adoptive T cell therapy has been cited 96 times in literature catalogued by pubmed, exceeding the typical impact factor of papers in the journal by four

times (Crompton et al., 2015). To its credit, the inhibition of AKT is used in one of the two FDA approved CAR-T methods of adoptive cell therapy; Yescarta®, developed by KITE Pharma (Johnson and June, 2017). Other companies focused on bringing CAR-T products to market also use AKT inhibitor, like Bluebird Bio, but their therapies are yet to receive approval for use (Perkins, et al., 2015).

6.2 T-cell Differentiation Through a non-apoptotic CD95 Signal

An understanding and delineation of the factors contributing to T cell differentiation had been elusive before the role of CD95 was uncovered (Klebanoff and Gattinoni, 2012). Just before the finding, it was noted that CD95 positivity was a marker for naive-like cells with high proliferative and self-renewing capacity (Gattinoni et al., 2011). The data presented in this thesis and the publications that followed, ascribe a central function to CD95 rather than a simple marker in the life cycle of a T cell (Leonardi AJ 2012, Klebanoff et al., 2016). Before, Fas was considered a canonical death receptor when pertaining to T cell function (Waring and Müllbacher, 1998). Now, a dual role has been delineated, showing naive and memory T cells have a tendency to differentiate with a Fas signal until they adopt an effector phenotype (Klebanoff et al., 2016). With further agonization of CD95 as an effector cell, they will then apoptose rather than remaining as memory (Klebanoff et al., 2016).

The publication in 2016 detailing the CD95 differentiation phenotype has been cited 53 times, more than twice that of other papers in the Journal of Clinical Investigation. These citations explore the concept of optimizing T cell function to better adoptive immunotherapy of cancer. A more direct application of this finding came from collaborators to the original work in the lab of Dr. Richard Siegel. Taking into account the information we passed to them in regard to this finding, they verified that patients with Autoimmune Lymphoproliferative Syndrome (ALPS), which is a syndrome where Fas is mutated, have T cells which are lower in AKT activity and do not differentiate when treated with Fas Ligand Trimer, contrary to normal T cells (Cruz et al., 2016). This is a novel insight into the pathogenesis of ALPS, but the finding has yet to translate into treatment due to lack of a point of reasonable mechanistic intervention.

6.3 Concluding Remarks and Future Consideration

The field of adoptive immunotherapy of cancer is rapidly growing, propelled by advancements that make the method more efficacious. It is now at the maturity to where it has become a viable method in the treatment of widely disseminated metastatic disease such as leukemias and lymphomas. Stepwise advances pertaining to the T cell's function are the "effector" arm of the field, consistently yielding increases in efficacy which promise the goal of complete responses. The experiments presented in this work are such advancements. On the basis of the data presented, it can be concluded that:

1) T cells have a differentiation mechanism via Fas that can act in a paracrine manner (Figures 4.1, 4.2, 4.3, Klebanoff et al., 2016).
2) Fas has two distinct functions that can be distinguished by a C194V mutation- death and differentiation (Figure 4.1, Klebanoff et al., 2016).
3) The Fas-mediated differentiation signal is dependent upon AKT and reciprocally, AKT inhibition prevents Fas- mediated differentiation (Figure 4.4) (Klebanoff et al., 2016).
4) Fas-mediated differenitation attenuates T cell adoptive immunotherapy efficacy and Fas blockade augments efficacy of cultures with mixed differentiation (Figure 4.5, Klebanoff et al., 2016).
5) AKT inhibition prevents the differentiation of T cells transduced with a CD19 CAR (Figure 4.6, Klebanoff et al., 2017).
6) AKT inhibition lowers the glycolytic activity of T cells transduced with a CD19 CAR (Figure 4.6, Klebanoff et al., 2017).
7) AKT inhibition promotes FOXO1 nuclear localization (Figure 4.8, Klebanoff et al., 2017).
8) FOXO1 expression maintains a T cell memory phenotype (Figure 4.9, Klebanoff et al., 2017).
9) AKT inhibition of CAR-T cells yields superior tumor treatment efficacy. (Figure 4.10, Klebanoff et al., 2017).

Inhibition of AKT is being applied in clinical trials of adoptive immunotherapy and is used in the first FDA-approved commercial adoptive T cell immunotherapy in the United States. Furthermore, the marked control of differentiation is not exclusive to AKT inhibition; Fas may be targeted as well. Given Fas' role in apoptosis however, care must be taken in an

approach which attenuates the death pathway, as cells could retain DNA damage or alterations that would normally prompt the Fas- dependent death pathway but are inhibited from doing so. In regards to FasL mediating T-cell differentiation, a FasL mimicking antibody or recombinant protein could be used which targets undifferentiated T cell malignancies in order to differentiate them. Also, to follow the path of investigation FOXO1 has illustrated, would cells with enforced FOXO1 activity treat tumor in concordance with the 62L expression it maintains on T cells? Such questions are well within the realm of practical investigation, and addressing them would further advance the field.

In summary, by investigating facets of T cell proliferation and differentiation, novel and practical methods of culturing T cells for adoptive immunotherapy have been found. These insights can be translated to more effective applications of adaptive T-cell immunotherapy for the management of cancer patients.

7 METHODOLOGY

7.1 Study Approval

Animal experiments were conducted with the approval of the NCI and NIAMS Animal Use and Care Committees. All anonymous NIH Blood Bank donors and cancer patients providing human samples were enrolled in clinical trials approved by the NIH Clinical Center and NCI institutional review boards. Each patient signed an informed consent form and received a patient information form prior to participation. Reproduced with permission from the Journal of Clinical Investigation (Klebanoff et al., 2016).

7.2 Cell Culture

Tumor cell lines were maintained in R10 medium, which consisted of RPMI 1640 medium (Lonza) supplemented with 10% FBS (Hyclone), penicillin/streptomycin (100 U ml–1/100 μG ml–1; Lonza), and 2 mM GlutaMAX (Invitrogen). T cells were maintained in T cell media, which consisted of AIMV (Invitrogen) supplemented with 5% human serum (Valley Biomedical), penicillin/streptomycin, nonessential amino acids (Gibco), GlutaMAX (Thermo Fisher Scientific), 0.055 mM 2-mercaptoethanol (Gibco), and 50 CU ml–1 of rhIL-2 (Novartis). Where indicated, cells were cultured continuously with indicated concentrations of AKTi (Calbiochem) dissolved in DMSO (MilliporeSigma). Reproduced with permission from the Journal of Clinical Investigation (Klebanoff et al., 2016).

7.3 Antibodies and Flow Cytometry

Mouse cells were stained with fluorochrome-conjugated antibodies against combinations of the following surface and intracellular antigens after Fc receptor blockade (2.4G2): CD8α (clone 53-6.7), CD27 (clone LG.3A10), CD44 (clone IM7), CD45.1(clone A20), CD45.2 (clone 104), CD62L (clone MEL-14), CD90.1 (clone OX-7), CD90.2 (clone 53-2.1), CD95 (clone Jo2), CD122 (clone TM–β1), CD178 (clone MFL3), IFN-γ (clone XMG1.2), KLRG-1 (clone 2F1), and Sca-1 (clone D7) (all purchased from BD Biosciences). Fluorochrome conjugates against pS6 S235/236 (D57.2.2E), pAKT T308

(C31E5E), and pAKT S473 (D9E) were obtained from Cell Signaling Technologies. Human cells were stained with combinations of the following fluorochrome-conjugated antibodies: CCR7 (150503), CD28 (CD28.2), CD45RO (UCHL1), CD8 (SK1) (BD Biosciences) or CD27 (M-T271), CD45RA (HI100), and CD62L (DREG-56) (BioLegend). Stimulation of T cells for intracellular cytokine staining was accomplished using Leukocyte Activation Cocktail containing phorbol myristate acetate and ionomycin in combination with brefeldin A and monensin solution (BD Biosciences). Apoptosis and specific cell death in defined T cell subsets was assessed using fluorochrome-conjugated annexin V and 7-AAD (both from BD Biosciences), as previously described (Abu Eid et al., 2015). Where indicated, TN-derived and TMem-derived subsets were reisolated for additional analyses by FACS sorting to greater than 92% purity using FACS sorting or magnetic bead isolation. Cell viability was determined using PI exclusion in FACS-sorting experiments or fixable live/dead cells (Invitrogen) for diagnostic experiments. For FACS–based glucose uptake assays, we incubated CD8+ T cells with 100 μM 2-NBDG (Invitrogen) for 2 hours before measuring by FACS, as previously described (Chandran et al., 2015). Flow cytometric data were acquired using either BD FACSCanto II, LSR, or LSRFortessa cytometers (BD Biosciences). FACS data, including calculation of PI, were analyzed with FlowJo Version 9.7 software (TreeStar). Reproduced with permission from the Journal of Clinical Investigation (Klebanoff et al., 2016).

7.4 Mouse Strains and Animal Studies

Adult (6 to 12 weeks old) female C57BL/6 (B6; Ly5.2+), B6.SJL-Ptprca Pep3b/BoyJ (Ly5.1+), B6.PL-Thy1a/CyJ (Thy1.1+), B6.MRL-Faslpr/J (lpr) (44), B6.129S7-Rag1tm1Mom/J (Rag), B6.Cg-Thy1a/Cy Tg(TcraTcrb)8Rest/J (pmel-1) (24), and B6-Tg(TcraTcrb)1100Mjb/J (OT-1) (Hedrick et al., 2012) CD8+ TCR transgenic mice were all purchased from the Jackson Laboratory. Transgenic mice harboring the Fas C194V mutant receptor were generated via BAC containing the Fas locus, with the C194V generated by recombineering. These mice were backcrossed to lpr mice on a B6 background. FasC194V lpr/lpr mice were backcrossed to homozygosity for both the lpr Fas allele and the C194V Fas transgene. Where indicated, pmel-1 and OT-1 mice were crossed to Thy1.1, Ly5.1, Rag, or Rag × lpr backgrounds. All mice were maintained under specific pathogen–free conditions. Reproduced with permission from the Journal of Clinical Investigation (Klebanoff et al., 2016).

7.5 Mouse Xenograft ACT Studies

Female NOD.Cg-Prkdcscid Il2rgtm1Wjl/SzJ (The Jackson Laboratory) mice were used at ≥ 6 weeks of age. Mice were inoculated by i.v. tail vein injection with 2 × 106 NALM6-GL cells. Three days later, mice were randomly assigned to receive either no T cells or 1 × 106 human anti-CD19 CAR–transduced T cells expanded in the presence or absence of AKTi administered by i.v injection. No exogenous cytokine support was administered following adoptive transfer. Tumor burden was evaluated using bioluminescent imaging with a Xenogen Spectrum system and Living Image v3.2 software following i.p. administration of 150 mg/kg of D-luciferin (Caliper Life Sciences). Reproduced with permission from JCI Insight (Klebanoff et al., 2017).

7.6 Xenografted Cell lines

The following CD19+ cell lines were used as positive controls: NALM6 (DSMZ), NALM6-GL (a previously described NALM6 line stably transduced with firefly luciferase) (Sabatino et al., 2016), and Toledo (ATCC). K562-CD19 (Kochenderfer et al., 2009) and 143B-CD19 (Long et al., 2015) (a gift from C.L. Mackall, Stanford University, Stanford, California, USA) are both CD19– tumor cell lines stably transduced with CD19. The following CD19– cell lines were used as negative controls: K562 (ATCC) and CEM (ATCC). Reproduced with permission from JCI Insight (Klebanoff et al., 2017).

7.7 Evaluation of vaccine-induced and antitumor immunity

Adult female B6 mice were implanted by s.c. injection with 4 × 105 B16 (H-2Db) cells, a spontaneous gp100+ murine melanoma cell line obtained from the NCI tumor repository. Ten days later, tumor-bearing mice received 6 Gy total body irradiation. Treated mice received i.v. injection of indicated doses and subsets of pmel-1 CD8+ T cells in combination with 2 × 107 pfu of a previously described recombinant vaccinia virus (rVV-gp100) (24) (rVV-gp100) and 12 μg IL-2 (Prometheus) administered twice daily by i.p. injection for a total of 6 doses. All tumor measurements were performed in a blinded

fashion. Reproduced with permission from the Journal of Clinical Investigation (Klebanoff et al., 2016).

7.8 Isolation and Generation of Mouse and Human CD8+ T Cell Subsets

Mouse TN cells were isolated either by using a MACS CD8+ negative selection kit (Miltenyi Biotech) in combination with a 1:300 dilution of biotin-conjugated anti-CD44 antibody or by FACS sorting CD44loCD62LhiCD8+ T cells using FACSAria (BD Biosciences). Mouse TMem cells were generated by in vitro differentiation (as previously described) or by adoptive transfer of congenically distinguishable Thy1.1+ or Ly5.1+ pmel-1 CD8+ T cells into Ly5.2+ WT mice, where recipient mice were vaccinated with rVV-gp100 (2 × 107 PFU) and vaccine-induced TCM (CD44hiCD62L+) or TEM (CD44hiCD62L–) adoptively transferred subsets were isolated by FACs sorting more than 28 days later (Macintyre et al., 2011, Sukumar et al., 2016). Human T cells were obtained either by leukapheresis or venipuncture and prepared over Ficoll-Hypaque gradient (LSM; ICN Biomedicals Inc.). Human TN cells and TMem cells were obtained by magnetic bead isolation using the EasySep Human Naive CD8+ T Cell and Memory CD8+ T Cell Enrichment Kits, respectively (STEMCELL Technologies). Fate tracking of TN and TMem cells was accomplished by labeling cells with Cell Proliferation Dye eFluor 450 and Cell Proliferation Dye eFluor 670, respectively (eBioscience). Reproduced with permission from the Journal of Clinical Investigation (Klebanoff et al., 2016).

7.9 Activation and expansion of CD8+ T cells

Both mouse and human TN cells with or without TMem cells were activated and expanded at indicated ratios in 96-well round-bottom plates coated with 2 μg/ml of CD3-specific and 1 μg/ml of soluble CD28-specific antibodies (clones 145-2C11 and 37.51; BD Biosciences) in culture media containing 5 ng/ml (mouse) or 20 ng/ml (human) of IL-2 at a final density of 1 × 105 cells/well. Where indicated, T cells were cultured with specified concentrations of lz-FasL, a previously described recombinant oligomerized form of FasL (Abu Eid et al., 2015), or 10 μg ml–1 of either a blocking antibody against FasL (MFL3; BD Biosciences) or IgG (A19-3; BioLegend). In some experiments, cells were also

cultured with 1 μM of AKT Inhibitor VIII (Calbiochem) dissolved in DMSO (Sigma-Aldrich). Where indicated, TN-derived and TMem-derived subsets were reisolated for additional analyses by FACS sorting to more than 95% purity using FACS sorting or magnetic bead isolation. Reproduced with permission from the Journal of Clinical Investigation (Klebanoff et al., 2016).

7.10 Isolation, Expansion, and Retroviral Transduction of Human T Cells with a Clinical-Grade CAR or TCR

Generation of anti-CD19 CAR–transduced human T cells was accomplished using a previously described manufacturing process identical to that currently used for prior and current human clinical trials (Kochenderfer et al., 2015). Briefly, unfractionated PBMC were obtained either by leukapheresis or venipuncture from healthy donors (HDs) or patients and prepared over Ficoll-Hypaque gradient (ICN Biomedicals Inc.). Cells were resuspended in IL-2 containing media (300 IU ml–1), and T cell proliferation was initiated using 50 ng ml–1 of anti-CD3 antibody (OKT3; OrthoBiotech). Alternatively, FACS-sorted T cell subsets were stimulated with anti-CD3/CD28 activator beads (Invitrogen) at 1:3 T cell/bead ratio. RetroNectin (Takara Bio Inc.) was applied to nontissue culture–coated 6-well plates using an established protocol (Johnson et al., 2009), followed by addition of a previously described MSCV-based splice-gagvector (MSGV) retrovirus encoding either the FMC63-28z CAR (Kochenderfer et al.,. 2009) or a HLA-A*02 restricted NY-ESO-1 TCR (Robbins et al., 2008). Two days after T cell stimulation, 2 ×106 stimulated PBMC/well were added to retrovirus-coated plates and subsequently cultured overnight at 37oC. The next day, the cells were returned to culture in T cell media. Countbright beads were spiked-in for the flow cytometric quantification of relative and absolute cell numbers (Invitrogen). Reproduced with permission from JCI Insight (Klebanoff et al., 2017).

7.11 Antigen-Specific Functional Assays of CAR-modified T Cells

Specific IFNγ release by anti-CD19 CAR–modified T cells was measured by ELISA assay (Pierce) from supernatants following overnight coculture at a 1:1 ratio with indicated CD19+ and CD19– target cell lines in IL-2–free/AKTi-free culture media. Intracellular

cytokine staining (ICS) and tumor cell cytolysis was measured after a 6-hour coculture in a 1:2 ratio of anti-CD19 CAR–modified T cells to indicated tumor cell lines. Tumor cell cytotoxicity by receptor-engineered T cells and calculation of the tumor-elimination index was performed as described elsewhere (Mastaglio et al., 2017). ICS was performed in the presence of 1 μl of Golgi Plug (BD Pharmingen). Cells were subsequently washed, stained for viability and cell surface markers, permeabilized according to the manufacturer's instructions using a Cytofix/Cytoperm kit (BD Biosciences), and stained using fluorochrome conjugated antibodies against IFNγ (clone RPA-T8; BioLegend) and IL-2 (clone MQ1-17H12; BD Biosciences). Evaluation of cytolysis by receptor-engineered T cells was performed as previously described (Mastaglio et al., 2017) and calculated as the antigen-specific tumor elimination index. Reproduced with permission from JCI Insight (Klebanoff et al., 2017).

7.12 Antibodies and Flow Cytometry of Human CAR-T Cells.

Cells were stained with fluorochrome-conjugated antibodies against combinations of the following surface antigens: CD3 (SK7), CD4 (RPA-T4), CD8 (SK1), and CD62L (DREG-56) (all from BD Biosciences); CD28 (CD28.2, eBioscience); LAG-3 (17B4, Enzo); PD1 (MIH-4, Invitrogen); and TIM-3 (344823, R&D Systems). Fluorochrome conjugates against phoshpo-S6 S235/236 (D57.2.2E), phospho-AKT T308 (C31E5E), and phospho-AKT S473 (D9E) were obtained from Cell Signaling Technologies. Detection of the mouse anti–human CD19 scFv as a measure of transduction efficiency was detected as previously described (Kochenderfer et al., 2009). Briefly, Fc receptors were blocked with polyclonal goat IgG (Invitrogen), followed by incubation at 4oC for 25 minutes with biotin-labeled goat anti–mouse F(ab)2 antibody (Jackson ImmunoResearch). Cells were then blocked with polyclonal mouse IgG (Invitrogen) and then stained with PE-labeled streptavidin (BD Biosciences). Flow cytometric data was acquired using a either a BD FACSCanto II or LSRFortessa cytometer (BD Biosciences). FACS-sorting was performed on a FACSAria (BD Biosciences). FACS data was analyzed with FlowJo Version 9.8.5 software (TreeStar Inc.). Reproduced with permission from JCI Insight (Klebanoff et al., 2017).

7.13 Cytokine Release Assays of Murine T Cells

We pulsed B6 splenocytes with indicated concentrations of hgp10025–33 peptide and incubated cells with TN-derived pmel-1 CD8+ T cells at a 1:1 ratio overnight at 37°C. Supernatants were analyzed for mouse IFN-γ by ELISA (R&D Systems). Reproduced with permission from the Journal of Clinical Investigation (Klebanoff et al., 2016).

7.14 qPCR and Western Blot

For qPCR analysis, CD8+ T cell subsets were FACS sorted directly into RNAprotect Cell Reagent, and RNA was extracted using the QiaShredders and RNeasy Mini Kits (all from QIAGEN). cDNA was synthesized using the High Capacity RNA-to-cDNA kit (Applied Biosystems), and qPCR was performed on an ABI 7500 Fast Instrument (Applied Biosystems). Gene expression was quantified using probes targeting Ccr7, Cd27, Gzmb, Il7ra, Klf2, Sell, Tbx21, Tcf7, Tfrc, and Prdm1 (Applied Biosystems). For Western blot analysis, CD8+ T cells were sorted into FCS and subsequently lysed in protease inhibitor containing RIPA buffer (Cell Signaling Technology). Protein was quantified using the Bio-Rad protein assay. We separated 30 μg of total protein on a 4% to 12% SDS-PAGE gel followed by standard immunoblotting with antibodies to pAKTT308 (C31E5E; Cell Signaling Technology), GAPDH (AB2302; EMD Millipore), and horseradish peroxidase–conjugated goat antibodies to mouse and rabbit IgG (sc-2005 and sc-2004; Santa Cruz Biotechnology Inc.). Blots were developed using chemiluminescence (Thermo Fisher Scientific) and acquired using the ChemiDoc system (Bio-Rad Laboratories). Reproduced with permission from JCI Insight (Klebanoff et al., 2017).

7.15 Metabolic Profiling

ECAR was measured at 37°C using a Seahorse XFe96 Analyzer (Seahorse Bioscience) in XF media (nonbuffered RPMI 1640 containing 25 mM glucose, 2 mM L-glutamine, and 1 mM sodium pyruvate) under basal conditions as previously described (Sukumar et al., 2013). For FACS-based glucose uptake assays, T cells were incubated with 100 μM 2-NBDG (Invitrogen) for 2 hours before measuring by FACS, also as previously described (Sukumar et al., 2013). T cells exposed to AKTi were maintained continuously in the presence of the inhibitor, including during incubation with 2-NBDG and during FACS analysis. Quantification of individual metabolites was accomplished using a combination

of GC/MS and LC/MS/MS platforms on CAR-modified T cells from 3 independent donors (Metabolon). Reproduced with permission from JCI Insight (Klebanoff et al., 2017).

7.16 Microarray Analysis of Human T Cells

Gene expression levels were determined using Human Gene 1.0 ST arrays (Affymetrix) according to the manufacturer's protocols. Total RNA (300 ng) was used as starting material for cRNA amplification using the WT Expression kit (Invitrogen) according the manufacturer's protocol. cDNA was reverse transcribed, fragmented, labeled using the GeneChip WT Terminal Labeling kit (Affymetrix), and hybridized on the arrays for 18 hours according to the manufacturer's directions. Arrays were stained and washed in the Fluidics Station 400 (Affymetrix) and scanned (Affymetrix 7G). Arrays data were imported into Partek Genomic Suite using RMA normalization after background subtraction. The expression and sequencing data discussed in this manuscript are deposited in NCBI's GEO database and is accessible through the GEO series accession number GSE98078. Reproduced with permission from JCI Insight (Klebanoff et al., 2017).

7.17 Confocal Immunofluorescence Imaging and Analysis

Fluorescence image z-stacks were collected using a 63× plan-apochromat (numerical aperture) oil immersion objective lens on a Zeiss LSM 880 laser scanning confocal microscope (Carl Zeiss Microscopy Inc.). Tiled images were acquired with 5% image overlap, an optical slice thickness of 0.9 um, 0.07 um x-y pixel size, and 0.44 um z-step size. The z-stack image tiles were stitched using the Zen blue (v2.3) software. The stitched images were analyzed using the ImarisCell image analysis software (v. 8.2.1, Bitplane Inc.), with the Hoechst counterstain used to mask the nuclear volume and the phalloidin stain used to mask the cytoplasmic volume. The same image processing and analysis parameters were used for each of the images within a dataset. The mean intensity of the respective fluorescence channels was measured within the nucleus and cytoplasm, and the ratio of cytoplasmic to nuclear mean intensity was calculated for the individual cells. The multichannel fluorescence confocal image z-stacks were analyzed using the ImarisCell volume reconstruction module of the Imaris software. Briefly, within the ImarisCell module, the "cell with single nucleus" criterion was used to segment the nuclear volume compared with the cell cytoplasmic volume. The Hoechst fluorescence channel was used

to segment the nucleus, whereas the phalloidin-Alexa Fluor 488 fluorescence channel was used to segment the cell cytoplasm. Segmentation was based primarily on intensity threshold for the respective channels above background. Background was calculated from the nonstained (no Hoechst and no phalloidin) negative control cells. From the 2 segmented compartments within the individual cells, the FOXO1 mean pixel intensity was measured in an automated fashion for both the nucleus and cytoplasm. The same parameters used for segmenting the cellular compartments were applied to all cells in the dataset, regardless of treatment assignment. Reproduced with permission from JCI Insight (Klebanoff et al., 2017).

7.18 Statistics

The products of perpendicular tumor diameters were plotted as the mean ± SEM for each data point, and tumor treatment graphs were compared by using the Wilcoxon rank sum test and analysis of animal survival assessed using a log-rank test. Regression analysis of the slope of tumor regression as a function of CD62L+ cells among Fas-modulated CD8+ T cells was performed as described previously (Gubser et al., 2013). For all other experiments, data were compared using either an unpaired 2-tailed Student's t test corrected for multiple comparisons by a Bonferroni adjustment or repeated measures 1-way ANOVA, as indicated. In all cases, P values of less than 0.05 were considered significant. Statistics were calculated using Prism 5 GraphPad software (GraphPad Software Inc.) For microarray data, 1-way ANOVA was used to identify differentially expressed genes among the 4 T cell subtypes, with a significant cut off for the positive FDR < 0.01. Differentially expressed probe sets were selected without specifying a fold change criterion. Reproduced with permission from the Journal of Clinical Investigation (Klebanoff et al., 2016).

8 REFERENCES

Abu Eid R, Friedman KM, Mkrtichyan M, Walens A, King W, Janik J, Khleif SN. Akt1 and -2 inhibition diminishes terminal differentiation and enhances central memory CD8(+) T-cell proliferation and survival. Oncoimmunology. 2015 Feb 3;4(5):e1005448.

Bollard C, et al. Cytotoxic T lymphocyte therapy for Epstein–Barr virus Hodgkin's disease. J. Exp. Med. 2004;200:1623–1633.

Boyman, O., & Sprent, J. (2012). The role of interleukin-2 during homeostasis and activation of the immune system. Nature Reviews Immunology(12), 180-190.

Chandran SS, Paria BC, Srivastava AK, Rothermel LD, Stephens DJ, Kammula US. Tumor-Specific Effector CD8+ T Cells That Can Establish Immunological Memory in Humans after Adoptive Transfer Are Marked by Expression of IL7 Receptor and c-myc. Cancer Res. 2015 Aug 15;75(16):3216-26. doi: 10.1158/0008-5472.CAN-15-0584.

Chaudhary B, Elkord E. Regulatory T Cells in the Tumor Microenvironment and Cancer Progression: Role and Therapeutic Targeting. Vaccines (Basel). 2016 Aug 6;4(3). pii: E28. doi: 10.3390/vaccines4030028.

Crompton JG, Narayanan M, Cuddapah S, Roychoudhuri R, Ji Y, Yang W, Patel SJ, Sukumar M, Palmer DC, Peng W, Wang E, Marincola FM, Klebanoff CA, Zhao K, Tsang JS, Gattinoni L, Restifo NP. Lineage relationship of CD8(+) T cell subsets is

revealed by progressive changes in the epigenetic landscape. Cell Mol Immunol. 2016 Jul;13(4):502-13. doi: 10.1038/cmi.2015.32.

Crompton JG, Sukumar M, Restifo NP. Uncoupling T-cell expansion from effector differentiation in cell-based immunotherapy. Immunol Rev. 2014 Jan;257(1):264-276. doi: 10.1111/imr.12135.

Crompton JG, Sukumar M, Roychoudhuri R, Clever D, Gros A, Eil RL, Tran E, Hanada K, Yu Z, Palmer DC, Kerkar SP, Michalek RD, Upham T, Leonardi A, Acquavella N, Wang E, Marincola FM, Gattinoni L, Muranski P, Sundrud MS, Klebanoff CA, Rosenberg SA, Fearon DT, Restifo NP. Akt inhibition enhances expansion of potent tumor-specific lymphocytes with memory cell characteristics. Cancer Res. 2015 Jan 15;75(2):296-305. doi: 10.1158/0008-5472.CAN-14-2277.

Cruz AC, Ramaswamy M, Ouyang C, Klebanoff CA, Sengupta P, Yamamoto TN, Meylan F, Thomas SK, Richoz N, Eil R, Price S, Casellas R, Rao VK, Lippincott-SchwartzJ, Restifo NP, Siegel RM. Fas/CD95 prevents autoimmunity independently of lipid raft localization and efficient apoptosis induction. Nat Commun. 2016 Dec 23;7:13895. doi: 10.1038/ncomms13895.

David Clever, R. R. (2016). Oxygen Sensing by T Cells Establishes an Immunologically Tolerant Metastatic Niche. Cell, 166(5), 1117–1131.

Davila ML, Riviere I, Wang X, Bartido S, Park J, Curran K, Chung SS, Stefanski J, Borquez-Ojeda O, Olszewska M, Qu J, Wasielewska T, He Q, Fink M, Shinglot H, Youssif M, Satter M, Wang Y, Hosey J, Quintanilla H, Halton E, Bernal Y, Bouhassira DC, Arcila ME, Gonen M, Roboz GJ, Maslak P, Douer D, Frattini MG,

Giralt S, Sadelain M, Brentjens R. Efficacy and toxicity management of 19-28z CAR T cell therapy in B cell acute lymphoblastic leukemia. Sci Transl Med. 2014 Feb 19;6(224):224ra25. doi: 10.1126/scitranslmed.3008226.

Donye Dominguez, C. Y. (2017). Exogenous IL-33 Restores Dendritic Cell Activation and Maturation in Established Cancer. The Journal of Immunology(3), 1365-1375.

Duault, C. (2017). IL-33-expanded human Vγ9Vδ2 T cells have anti-lymphoma effect in a mouse tumor model. European Journal of Immunology, [Epub ahead of print].

Dudley ME, Wunderlich JR, Robbins PF, Yang JC, Hwu P, Schwartzentruber DJ, Topalian SL, Sherry R, Restifo NP, Hubicki AM, Robinson MR, Raffeld M, Duray P, Seipp CA, Rogers-Freezer L, Morton KE, Mavroukakis SA, White DE, Rosenberg SA. Cancer regression and autoimmunity in patients after clonal repopulation with antitumor lymphocytes. Science. 2002 Oct 25;298(5594):850-4. Epub 2002 Sep 19.

Dudley ME, Yang JC, Sherry R, Hughes MS, Royal R, Kammula U, Robbins PF, Huang J, Citrin DE, Leitman SF, Wunderlich J, Restifo NP, Thomasian A, Downey SG, Smith FO, Klapper J, Morton K, Laurencot C, White DE, Rosenberg SA. Adoptive cell therapy for patients with metastatic melanoma: evaluation of intensive myeloablative chemoradiation preparative regimens. J Clin Oncol. 2008 Nov 10;26(32):5233-9. doi: 10.1200/JCO.2008.16.5449.

Dunn GP, Old LJ, Schreiber RD. The immunobiology of cancer immunosurveillance and immunoediting. Immunity. 2004 Aug;21(2):137-48.

Eid, R. A., Ahmad, S., Lin, Y., Webb, M., Berrong, Z., Shrimali, R., . . . Khleif, S. N. (2017). Enhanced therapeutic efficacy and memory of tumor-specific CD8 T cells by ex vivo PI3K-δ inhibition. Cancer Research, 77(15), 4135-4145.

Frauwirth, K. A., Riley, J. L., Harris, M. H., Parry, R. V., Rathmell, J. C., Plas, D. R., . . . Thompson, C. B. (2002). The CD28 Signaling Pathway Regulates Glucose Metabolism. Immunity, 16(6), 769-777.

Gattinoni L, Finkelstein SE, Klebanoff CA, Antony PA, Palmer DC, Spiess PJ, Hwang LN, Yu Z, Wrzesinski C, Heimann DM, Surh CD, Rosenberg SA, Restifo NP. Removal of homeostatic cytokine sinks by lymphodepletion enhances the efficacy of adoptively transferred tumor-specific CD8+ T cells. J Exp Med. 2005 Oct 3;202(7):907-12.

Gattinoni L, Lugli E, Ji Y, Pos Z, Paulos CM, Quigley MF, Almeida JR, Gostick E, Yu Z, Carpenito C, Wang E, Douek DC, Price DA, June CH, Marincola FM, Roederer M, Restifo NP. A human memory T cell subset with stem cell-like properties. Nat Med. 2011 Sep 18;17(10):1290-7. doi: 10.1038/nm.2446.

Gattinoni L, Klebanoff CA, Restifo NP. Paths to stemness: building the ultimate antitumour T cell. Nat Rev Cancer. 2012 Oct;12(10):671-84. doi: 10.1038/nrc3322.

Gubser PM, Bantug GR, Razik L, Fischer M, Dimeloe S, Hoenger G, Durovic B, Jauch A, Hess C. Rapid effector function of memory CD8+ T cells requires an

immediate-early glycolytic switch. Nat Immunol. 2013 Oct;14(10):1064-72. doi: 10.1038/ni.2687.

Hedrick SM, Hess Michelini R, Doedens AL, Goldrath AW, Stone EL. FOXO transcription factors throughout T cell biology. Nat Rev Immunol. 2012 Sep;12(9):649-61. doi: 10.1038/nri3278.

Hendriks J, Gravestein LA, Tesselaar K, van Lier RA, Schumacher TN, Borst J. CD27 is required for generation and long-term maintenance of T cell immunity. Nat Immunol. 2000 Nov;1(5):433-40.

Hinrichs CS, Borman ZA, Gattinoni L, Yu Z, Burns WR, Huang J, Klebanoff CA, Johnson LA, Kerkar SP, Yang S, Muranski P, Palmer DC, Scott CD, Morgan RA, Robbins PF, Rosenberg SA, Restifo NP. Human effector CD8+ T cells derived from naive rather than memory subsets possess superior traits for adoptive immunotherapy. Blood. 2011 Jan 20;117(3):808-14. doi:10.1182/blood-2010-05-286286.

Hinrichs CS, Rosenberg SA. Exploiting the curative potential of adoptive T-cell therapy for cancer. Immunol Rev. 2014 Jan;257(1):56-71. doi:10.1111/imr.12132.

Johnson, C. B., Wrangle, J., Mehrotra, S., Li, Z., Paulos, C. M., Cole, D. J., . . . Rubinstein, M. P. (2016). Harnessing the IL-7/IL-7Rα axis to improve tumor immunotherapy. OncoImmunology, 5(5).

Johnson LA, Morgan RA, Dudley ME, Cassard L, Yang JC, Hughes MS, Kammula US, Royal RE, Sherry RM, Wunderlich JR, Lee CC, Restifo NP, Schwarz SL, Cogdill AP,

Bishop RJ, Kim H, Brewer CC, Rudy SF, VanWaes C, Davis JL, Mathur A, Ripley RT, Nathan DA, Laurencot CM, Rosenberg SA. Gene therapy with human and mouse T-cell receptors mediates cancer regression and targets normal tissues expressing cognate antigen. Blood. 2009 Jul 16;114(3):535-46. doi: 10.1182/blood-2009-03-211714.

Johnson, L. A., & June, C. H. (2017). Driving gene-engineered T cell immunotherapy of cancer. Cell Research, 27(1), 38-58.

Kawalekar OU, O'Connor RS, Fraietta JA, Guo L, McGettigan SE, Posey AD Jr, Patel PR, Guedan S, Scholler J, Keith B, Snyder NW, Blair IA, Milone MC, June CH. Distinct Signaling of Coreceptors Regulates Specific Metabolism Pathways and Impacts Memory Development in CAR T Cells. Immunity. 2016 Feb 16;44(2):380-90. doi: 10.1016/j.immuni.2016.01.021.

Kerkar, S. P., Leonardi, A. J., Panhuys, N. v., Zhang, L., Yu, Z., Crompton, J. G., . . . Restifo, N. P. (2013). Collapse of the Tumor Stroma is Triggered by IL-12 Induction of Fas. Molecular Therapy, 21(7), 1369-1377.

Kerkar SP, Goldszmid RS, Muranski P, Chinnasamy D, Yu Z, Reger RN, Leonardi AJ, Morgan RA, Wang E, Marincola FM, Trinchieri G, Rosenberg SA, Restifo NP. IL-12 triggers a programmatic change in dysfunctional myeloid-derived cells within mouse tumors. J Clin Invest. 2011 Dec;121(12):4746-57. doi: 10.1172/JCI58814.

Kershaw MH, Westwood JA, Parker LL, Wang G, Eshhar Z, Mavroukakis SA, White DE, Wunderlich JR, Canevari S, Rogers-Freezer L, Chen CC, Yang JC, Rosenberg SA, Hwu P. A phase I study on adoptive immunotherapy using gene-modified T cells for ovarian cancer. Clin Cancer Res. 2006 Oct 15;12(20 Pt 1):6106-15.

Klebanoff, C. A., Finkelstein, S. E., Surman, D. R., Lichtman, M. K., Gattinoni, L., Theoret, M. R., . . . Restifo, N. P. (2004). IL-15 enhances the in vivo antitumor activity of tumor-reactive CD8+ T cells. Proceedings of the National Academy of Sciences of the United States of America, 101(7), 1969-1974.

Klebanoff, C. A., Spencer, S. P., Torabi-Parizi, P., Grainger, J. R., Roychoudhuri, R., Ji, Y., . . . Restifo, N. P. (2013). Retinoic acid controls the homeostasis of pre-cDC–derived splenic and intestinal dendritic cells. Journal of Experimental Medicine, 210(10), 1961-1976.

Klebanoff CA*, Crompton JG*, Leonardi AJ*, Yamamoto TN, Chandran SS, Eil RL, Sukumar M, Vodnala SK, Hu J, Ji Y, Clever D, Black MA, Gurusamy D, Kruhlak MJ, Jin P, Stroncek DF, Gattinoni L, Feldman SA, Restifo NP. Inhibition of AKT signaling uncouples T cell differentiation from expansion for receptor-engineered adoptive immunotherapy. JCI Insight. 2017 Dec 7;2(23). pii: 95103. doi: 10.1172/jci.insight.95103. *= co-first authorship.

Klebanoff CA*, Scott CD*, Leonardi AJ*, Yamamoto TN, Cruz AC, Ouyang C, Ramaswamy M, Roychoudhuri R, Ji Y, Eil RL, Sukumar M, Crompton JG, Palmer DC, Borman ZA, Clever D, Thomas SK, Patel S, Yu Z, Muranski P, Liu H, Wang E, Marincola FM, Gros A, Gattinoni L, Rosenberg SA, Siegel RM, Restifo NP. Memory T cell-driven

differentiation of naive cells impairs adoptive immunotherapy. J Clin Invest. 2016 Jan;126(1):318-34. doi: 10.1172/JCI81217. *= co-first authorship.

Kochenderfer JN, Feldman SA, Zhao Y, Xu H, Black MA, Morgan RA, Wilson WH, Rosenberg SA. Construction and preclinical evaluation of an anti-CD19 chimeric antigen receptor. J Immunother. 2009 Sep;32(7):689-702. doi: 10.1097/CJI.0b013e3181ac6138.

Kochenderfer JN, Dudley ME, Kassim SH, Somerville RP, Carpenter RO, Stetler-Stevenson M, Yang JC, Phan GQ, Hughes MS, Sherry RM, Raffeld M, Feldman S, Lu L, Li YF, Ngo LT, Goy A, Feldman T, Spaner DE, Wang ML, Chen CC, Kranick SM, Nath A, Nathan DA, Morton KE, Toomey MA, Rosenberg SA. Chemotherapy-refractory diffuse large B-cell lymphoma and indolent B-cell malignancies can be effectively treated with autologous T cells expressing an anti-CD19 chimeric antigen receptor. J Clin Oncol. 2015 Feb 20;33(6):540-9. doi: 10.1200/JCO.2014.56.2025.

Kolb HJ, Mittermüller J, Clemm C, Holler E, Ledderose G, Brehm G, Heim M, Wilmanns W. Donor leukocyte transfusions for treatment of recurrent chronic myelogenous leukemia in marrow transplant patients. Blood. 1990 Dec 15;76(12):2462-5.

Lasek, W., & Zagozdzon, R. (2016). Interleukin 12: Antitumor Activity and Immunotherapeutic Potential in Oncology. SpringerBriefs in Immunology.

Lasek, W., Zagozdzon, R., & Jakóbisiak, M. (2014). Interleukin 12: still a promising candidate for tumor immunotherapy? Cancer Immunology, Immunotherapy, 63(5), 419-435.

Lemery S, Keegan P, Pazdur R. First FDA Approval Agnostic of Cancer Site - When a Biomarker Defines the Indication. N Engl J Med. 2017 Oct 12;377(15):1409-1412. doi: 10.1056/NEJMp1709968.

Long AH, Haso WM, Shern JF, Wanhainen KM, Murgai M, Ingaramo M, Smith JP, Walker AJ, Kohler ME, Venkateshwara VR, Kaplan RN, Patterson GH, Fry TJ, Orentas RJ, Mackall CL. 4-1BB costimulation ameliorates T cell exhaustion induced by tonic signaling of chimeric antigen receptors. Nat Med. 2015 Jun;21(6):581-90. doi: 10.1038/nm.3838.

Macintyre AN, Finlay D, Preston G, Sinclair LV, Waugh CM, Tamas P, Feijoo C, Okkenhaug K, Cantrell DA. Protein kinase B controls transcriptional programs that direct cytotoxic T cell fate but is dispensable for T cell metabolism. Immunity. 2011 Feb 25;34(2):224-36. doi: 10.1016/j.immuni.2011.01.012.

Robbins PF, Li YF, El-Gamil M, Zhao Y, Wargo JA, Zheng Z, Xu H, Morgan RA, Feldman SA, Johnson LA, Bennett AD, Dunn SM, Mahon TM, Jakobsen BK, Rosenberg SA.
Single and dual amino acid substitutions in TCR CDRs can enhance antigen-specific T cell functions. J Immunol. 2008 May 1;180(9):6116-31.

Mineharu, Y., Kamran, N., Lowenstein, P. R., & Castro, M. G. (2014). Blockade of mTOR Signaling via Rapamycin Combined with Immunotherapy Augments Antiglioma Cytotoxic and Memory T-Cell Functions. Molecular Cancer Therapeutics, 13(12), 3024-3036.

Morgan RA, Dudley ME, Wunderlich JR, Hughes MS, Yang JC, Sherry RM, Royal RE, Topalian SL, Kammula US, Restifo NP, Zheng Z, Nahvi A, de Vries CR, Rogers-Freezer LJ, Mavroukakis SA, Rosenberg SA. Cancer regression in patients after transfer of genetically engineered lymphocytes. Science. 2006 Oct 6;314(5796):126-9. Epub 2006 Aug 31. PubMed PMID: 16946036; PubMed Central PMCID:
PMC2267026.

Neelapu SS, Tummala S, Kebriaei P, Wierda W, Gutierrez C, Locke FL, Komanduri KV, Lin Y, Jain N, Daver N, Westin J, Gulbis AM, Loghin ME, de Groot JF, Adkins S, Davis SE1, Rezvani K, Hwu P, Shpall EJ. Chimeric antigen receptor T-cell therapy - assessment and management of toxicities. Nat Rev Clin Oncol. Jan;15(1):47-62. (2018).

Orlowski RJ, Porter DL, Frey NV. The promise of chimeric antigen receptor T cells (CARTs) in leukaemia. Br J Haematol. 2017 Apr;177(1):13-26. doi:10.1111/bjh.14475.

Pearce EL, Walsh MC, Cejas PJ, Harms GM, Shen H, Wang LS, Jones RG, Choi Y. Enhancing CD8 T-cell memory by modulating fatty acid metabolism. Nature. 2009;460:103–7. doi: 10.1038/nature08097.

Pardoll DM. The blockade of immune checkpoints in cancer immunotherapy. Nat Rev Cancer. 2012 Mar 22;12(4):252-64. doi: 10.1038/nrc3239.

Perkins MR, Grande S, Hamel A, Horton HM, Garrett TE, Miller SM, Latimer IV HJ, Horvath CJ, Kuczewski M, Friedman KM, Morgan RA. Manufacturing an Enhanced CAR T Cell Product By Inhibition of the PI3K/Akt Pathway During T Cell Expansion Results in Improved In Vivo Efficacy of Anti-BCMA CAR T Cells. Blood 2015 126:1893

Radvanyi LG. Tumor-Infiltrating Lymphocyte Therapy: Addressing Prevailing Questions. Cancer J. 2015 Nov-Dec;21(6):450-64. doi:10.1097/PPO.0000000000000162.
Robert Eil, S. K. (2017). Ionic immune suppression within the tumour microenvironment limits T cell effector function. Nature(7621), 539-543.

Riddell SR, Sommermeyer D, Berger C, Liu LS, Balakrishnan A, Salter A, Hudecek M, Maloney DG, Turtle CJ. Adoptive therapy with chimeric antigen receptor-modified T cells of defined subset composition. Cancer J. 2014 Mar-Apr;20(2):141-4. doi: 10.1097/PPO.0000000000000036.

Robbins PF, Li YF, El-Gamil M, Zhao Y, Wargo JA, Zheng Z, Xu H, Morgan RA, Feldman SA, Johnson LA, Bennett AD, Dunn SM, Mahon TM, Jakobsen BK, Rosenberg SA.
Single and dual amino acid substitutions in TCR CDRs can enhance antigen-specific T cell functions. J Immunol. 2008 May 1;180(9):6116-31.

Rooney CM, Smith CA, Ng CY, Loftin SK, Sixbey JW, Gan Y, Srivastava DK, Bowman LC, Krance RA, Brenner MK, Heslop HE. Infusion of cytotoxic T cells for the prevention and treatment of Epstein-Barr virus-induced lymphoma in allogeneic transplant recipients. Blood. 1998 Sep 1;92(5):1549-55.

Rosenberg, S. A., Packard, B. S., Aebersold, P. M., Solomon, D., Topalian, S. L., Toy, S. T., . . . White, D. E. (1988). Use of Tumor-Infiltrating Lymphocytes and Interleukin-2 in the Immunotherapy of Patients with Metastatic Melanoma. New England Journal of Medicine, 319, 1676-1680.

Rosenberg SA, Restifo NP, Yang JC, Morgan RA, Dudley ME. Adoptive cell transfer: a clinical path to effective cancer immunotherapy. Nat Rev Cancer. 2008 Apr;8(4):299-308. doi: 10.1038/nrc2355.

Rosenberg SA, Yang JC, Sherry RM, Kammula US, Hughes MS, Phan GQ, Citrin DE, Restifo NP, Robbins PF, Wunderlich JR, Morton KE, Laurencot CM, Steinberg SM, White DE, Dudley ME. Durable complete responses in heavily pretreated patients with metastatic melanoma using T-cell transfer immunotherapy. Clin Cancer Res. 2011 Jul 1;17(13):4550-7. doi: 10.1158/1078-0432.CCR-11-0116. Epub 2011 Apr 15.

Rubinstein, M. P., Cloud, C. A., Garrett, T., Moore, C. J., Schwartz, K. M., Johnson, C. B., . . . Cole, D. J. (2012). Ex Vivo Interleukin-12-Priming During CD8+ T Cell Activation Dramatically Improves Adoptive T Cell Transfer Antitumor Efficacy in a Lymphodepleted Host. Journal of The American College of Surgeons, 214(4), 700-707.

Sabatino M, Hu J, Sommariva M, Gautam S, Fellowes V, Hocker JD, Dougherty S, Qin H, Klebanoff CA, Fry TJ, Gress RE, Kochenderfer JN, Stroncek DF, Ji Y, Gattinoni L. Generation of clinical-grade CD19-specific CAR-modified CD8+ memory stem cells for the treatment of human B-cell malignancies. Blood. 2016 Jul 28;128(4):519-28. doi: 10.1182/blood-2015-11-683847.

Sneller MC, Kopp WC, Engelke KJ, Yovandich JL, Creekmore SP, Waldmann TA, Lane HC. IL-15 administered by continuous infusion to rhesus macaques induces massive expansion of CD8+ T effector memory population in peripheral blood. Blood. 2011 Dec 22;118(26):6845-8. doi: 10.1182/blood-2011-09-377804.

Sukumar, M., & Gattinoni, L. (2014). The short and sweet of T-cell therapy: Restraining glycolysis enhances the formation of immunological memory and antitumor immune responses. OncoImmunology, 3(1).

Sukumar, M., Liu, J., Ji, Y., Subramanian, M., Crompton, J. G., Yu, Z., . . . Gattinoni, L. (2013). Inhibiting glycolytic metabolism enhances CD8+ T cell memory and antitumor function. Journal of Clinical Investigation, 123(10), 4479-4488.

Sukumar, M., Liu, J., Mehta, G. U., Patel, S. J., Roychoudhuri, R., Crompton, J. G., . . . Restifo, N. P. (2016). Mitochondrial Membrane Potential Identifies Cells with Enhanced Stemness for Cellular Therapy. Cell Metabolism, 23(1), 63-76.

Svane IM, Verdegaal EM. Achievements and challenges of adoptive T cell therapy with tumor-infiltrating or blood-derived lymphocytes for metastatic melanoma: what is needed to achieve standard of care? Cancer Immunol Immunother. 2014 Oct;63(10):1081-91. doi: 10.1007/s00262-014-1580-5.

Turtle CJ, Riddell SR. Genetically retargeting CD8+ lymphocyte subsets for cancer immunotherapy. Curr Opin Immunol. 2011 Apr;23(2):299-305. doi: 10.1016/j.coi.2010.12.012.

van der Windt GJ, Pearce EL. Metabolic switching and fuel choice during T-cell differentiation and memory development. Immunol Rev. 2012 Sep;249(1):27-42. doi: 10.1111/j.1600-065X.2012.01150.x.

Vinay DS, Ryan EP, Pawelec G, Talib WH, Stagg J, Elkord E, Lichtor T, Decker WK, Whelan RL, Kumara HMCS, Signori E, Honoki K, Georgakilas AG, Amin A, Helferich WG, Boosani CS, Guha G, Ciriolo MR, Chen S, Mohammed SI, Azmi AS, Keith WN, Bilsland A, Bhakta D, Halicka D, Fujii H, Aquilano K, Ashraf SS, Nowsheen S, Yang X, Choi BK, Kwon BS. Immune evasion in cancer: Mechanistic basis and therapeutic strategies. Semin Cancer Biol. 2015 Dec;35 Suppl:S185-S198. doi: 10.1016/j.semcancer.2015.03.004.

Vizcardo R, Klemen ND, Islam SMR, Gurusamy D, Tamaoki N, Yamada D, Koseki H, Kidder BL, Yu Z, Jia L, Henning AN, Good ML, Bosch-Marce M, Maeda T, Liu C, Abdullaev Z, Pack S, Palmer DC, Stroncek DF, Ito F, Flomerfelt FA, Kruhlak MJ, Restifo NP. Generation of Tumor Antigen-Specific iPSC-Derived Thymic Emigrants Using a 3D Thymic Culture System. Cell Rep. 2018 Mar 20;22(12):3175-3190. doi: 10.1016/j.celrep.2018.02.087.

Wallen H, Thompson JA, Reilly JZ, Rodmyre RM, Cao J, Yee C. Fludarabine modulates immune response and extends in vivo survival of adoptively transferred CD8 T cells in patients with metastatic melanoma. PLoS One. 2009;4(3):e4749. doi: 10.1371/journal.pone.0004749.

Waring P, Müllbacher A. Cell death induced by the Fas/Fas ligand pathway and its role in pathology. Immunol Cell Biol. 1999 Aug;77(4):312-7.

Watkins TS, Miles JJ. Tracking the T-cell repertoire after adoptive therapy. Clin Transl Immunology. 2017 May 5;6(5):e140. doi: 10.1038/cti.2017.16.

APPENDIX 1 RELEVANT PUBLICATIONS

Kerkar, SP, Goldszmid, RS, Muranski, P, Chinnasamy, D, Yu, Z, Reger, RM, **Leonardi, AJ**, Morgan, RA, Wang, E, Marincola, FM, Trinchieri, G, Rosenberg, SA, & Restifo, NP (2011). IL-12 triggers a programmatic change in dysfunctional myeloid-derived cells within mouse tumors. *J Clin Invest*., 2011 Dec;121(12):4746-57

Anthony J. Leonardi & Joseph G. Crompton. AKT Inhibition Uncouples Proliferation and Differentiation in Stimulated CD8+ T-Cells. Clinical Cancer Research FYI Colloquium, National Institutes of Health in Bethesda, Maryland. March 26, 2012.

Anthony J. Leonardi. Fas receptor stimulation causes CD8+ T Cell differentiation. NIH Postbac poster day. National Institutes of Health in Bethesda, Maryland. April 25, 2012.

Leonardi AJ, Klebanoff CA, Gattinoni LG, Restifo NP. Exposing T Cells to Fas Ligand (FasL)- Fas Receptor (FasR) Antagonists Withholds Differentiation and Increases Expansion Making T-cells More Suitable for Use in Cancer Immunotherapy. Federal Register. 2012 July 6. 40073-40076. https://www.federalregister.gov/documents/2012/07/06/2012-16500/government-owned-inventions-availability-for-licensing

Klebanoff CA, Spencer SP, Torabi-Parizi P, Grainger JR, Roychoudhuri R, Ji Y, Sukumar M, Muranski P, Scott CD, Hall JA, Ferreyra GA, **Leonardi AJ**, Borman ZA, Wang J, Palmer DC, Wilhelm C, Cai R, Sun J, Napoli JL, Danner RL, Gattinoni L, Belkaid Y, Restifo NP. Retinoic acid controls the homeostasis of pre-cDC-derived splenic and intestinal dendritic cells. J Exp Med. 2013 Sep 23;210(10):1961-76. doi: 10.1084/jem.20122508.

Kerkar, S. P., **Leonardi, A. J**., Panhuys, N. v., Zhang, L., Yu, Z., Crompton, J. G., . . . Restifo, N. P. (2013). Collapse of the Tumor Stroma is Triggered by IL-12 Induction of Fas. Molecular Therapy, 21(7), 1369-1377.

Crompton JG, Sukumar M, Roychoudhuri R, Clever D, Gros A, Eil RL, Tran E, Hanada K, Yu Z, Palmer DC, Kerkar SP, Michalek RD, Upham T, **Leonardi A**, Acquavella N, Wang E, Marincola FM, Gattinoni L, Muranski P, Sundrud MS, Klebanoff CA, Rosenberg SA, Fearon DT, Restifo NP. Akt inhibition enhances expansion of potent tumor-specific lymphocytes with memory cell characteristics. *Cancer Res*. 2015 Jan 15;75(2):296-305. doi: 10.1158/0008-5472.CAN-14-2277.

Tori Yamamoto, **Anthony Leonardi**, Hui Liu, Ena Wang, Luca Gattinoni, Anthony Cruz, Claudia Ouyang, Richard Siegel, Nicholas Restifo, and Christopher A Klebanoff. Fas expression in memory CD8+ T cell subsets augments cellular differentiation and effector function. 30th Annual Meeting and Associated Programs of the Society for Immunotherapy of Cancer (SITC 2015) National Harbor, MD, USA. November 4-8, 2015.

Klebanoff CA*, Scott CD*, **Leonardi AJ***, Yamamoto TN, Cruz AC, Ouyang C, Ramaswamy M, Roychoudhuri R, Ji Y, Eil RL, Sukumar M, Crompton JG, Palmer DC, Borman ZA, Clever D, Thomas SK, Patel S, Yu Z, Muranski P, Liu H, Wang E, Marincola FM, Gros A, Gattinoni L, Rosenberg SA, Siegel RM, Restifo NP. Memory T cell–driven differentiation of naive cells impairs adoptive immunotherapy *J Clin Invest*. 2016 Jan 4;126(1):318-34. doi: 10.1172/JCI81217. *= denotes co-first authorship

Klebanoff CA*, Crompton JG*, **Leonardi AJ*,** Yamamoto TN, Chandran SS, Eil RL, Sukumar M, Vodnala SK, Hu J, Ji Y, Clever D, Black MA, Gurusamy D, Kruhlak MJ, Jin P, Stroncek DF, Gattinoni L, Feldman SA, Restifo NP. Inhibition of AKT signaling uncouples T cell differentiation from expansion for receptor-engineered adoptive immunotherapy. JCI Insight. 2017 Dec 7;2(23). pii: 95103. doi: 10.1172/jci.insight.95103. *= denotes co-first authorship

Anthony J Leonardi. Immunotherapies combined with TNFa signaling modulators. International patent application WO2018045069. March 8, 2018.

Remaining pages removed due to copyright reasons